

**ATTENUATION RELATIONSHIP BASED ON STRONG MOTION DATA
RECORDED IN TURKEY**

EROL KALKAN

DECEMBER 2001

**ATTENUATION RELATIONSHIP BASED ON STRONG MOTION DATA
RECORDED IN TURKEY**

**A THESIS SUBMITTED TO
THE GRADUATE SCHOOL OF NATURAL AND APPLIED SCIENCES
OF
THE MIDDLE EAST TECHNICAL UNIVERSITY**

BY

EROL KALKAN

**IN PARTIAL FULFILLMENT OF THE REQUIREMENTS FOR THE DEGREE OF
MASTER OF SCIENCE
IN
THE DEPARTMENT OF CIVIL ENGINEERING**

DECEMBER 2001

Approval of the Graduate School of Natural and Applied Sciences

Prof.Dr. Tayfur ÖZTÜRK
Director

I certify that this thesis satisfies all the requirements as a thesis for the degree of
Master of Science.

Prof.Dr. Mustafa TOKYAY
Head of Department

This is to certify that we have read this thesis and that in our opinion it is fully adequate, in
scope and quality, as a thesis for the degree of Master of Science.

Prof.Dr. Polat GÜLKAN
Supervisor

Examining Committee Members

Prof.Dr. Polat GÜLKAN

Prof.Dr. Haluk SUCUOĞLU

Assoc.Prof.Dr. Can BALKAYA

Assoc.Prof.Dr. Azer KERİMOV

Dr. Engin KARAESMEN

ABSTRACT

ATTENUATION RELATIONSHIP BASED ON STRONG MOTION DATA RECORDED IN TURKEY

KALKAN, Erol

M.S., Department of Civil Engineering

Supervisor: Prof.Dr. Polat Gülkan

December 2001, 78 pages

Estimation of ground motion, either through the use of special earthquake codes or more specifically from site-specific researches is essential for the design of engineered structures. Rarely there are a sufficient number of ground-motion recordings near a site to allow a direct empirical estimation of the future motions expected for a design earthquake. Therefore it is necessary to develop attenuation relationship expressed in the form of equations or graphical curves for estimation ground motions in terms of magnitude, distance, site conditions and other effecting parameters. This is essential for both site-specific design and regional earthquake hazard mapping.

Today there exist no reliable attenuation relationships published for Turkey in the international scientific literature. To address this deficiency one of the attenuation relationships derived on the basis of western North American Earthquakes by Boore et al. (1997), is selected in this study as a model, and valid mathematical formula is calculated by the help of nonlinear regression analysis on the basis of actual earthquake recordings taken in Turkey. This formula relating the selected ground-motion parameter of peak ground acceleration as well as spectral values of

the same variable to the different factors that influence the value of this parameter.

The results of the analyses show that use of these predictive equations for the prediction of PGA and spectral acceleration values is a useful tool to construct site geology, distance and magnitude dependent response spectra for possible use in design, for any earthquake zone in Turkey. The results are compared with the site-dependent response spectral shapes prescribed in the 1997 Uniform Building Code (UBC) and current Turkish Seismic Code. It is shown that current design spectra in Turkey are too conservative for most structures located at distances from the active faults greater than 10 km. The results demonstrate that given response spectra models provide an accurate prediction of site and region-dependent ground-motion design parameters for a broad range of earthquake magnitudes, distances and geological conditions and may be used as an efficient tool both in deterministic (scenario earthquakes) and probabilistic seismic hazard assessment. These comparisons clearly serve as a reminder that there exists little support for the carefree import of design spectra curves from other environments for use in important engineering applications elsewhere.

Keywords: Attenuation relationship, earthquake hazard, nonlinear regression analysis, site-dependent response spectra, shear wave velocity

ÖZ

GÜÇLÜ DEPREM KAYITLARI KULLANILARAK TÜRKİYE İÇİN GEÇERLİ BİR AZALIM İLİŞKİSİNİN BULUNMASI

KALKAN, Erol

Yüksek Lisans, İnşaat Mühendisliği Bölümü

Tez Yöneticisi: Prof.Dr. Polat Gülkan

Aralık 2001, 78 sayfa

Mühendis yapılarının dizaynında özellikle deprem standartlarının kullanılması ya da bilimsel saha araştırmaları ile oluşabilecek deprem hareketlerinin tahmini vazgeçilmez derecede gereklidir. Yakın çevrede yeterli derecede yer hareketi kayıtlarının elde edilmesi o bölgede oluşabilecek depremlerin tahmininde kullanılabilir fakat yeterli miktarda kayıt bulunması oldukça nadir bir durum olarak karşımıza çıkmaktadır. Bu nedenle yer hareketinin, magnitüd, mesafe, saha jeolojisi ve diğer etkili parametreler cinsinden tanımlanmış, denklem ve grafik eğriler halinde geçerli bir azalım ilişkisinin bulunması gerekmektedir. Böyle bir ilişki hem belirli bölgelerde yapılacak yapıların hesabında hem de bölgesel deprem risk haritalarında kullanılabilir.

Günümüzde, Türkiye için geçerli olan ve uluslararası bilimsel çevrelerde yayınlanmış bir azalım ilişkisi bulunmamaktadır. Bu nedenle Boore et al. (1997)'nin Kuzey Batı Amerika depremlerini baz alarak belirlemiş oldukları azalım ilişkisi bu tez çalışması için model olarak kabul edilmiş ve bu model doğrultusunda Türkiye'de kaydı alınan deprem hareketlerinin doğrusal olmayan regresyon analizi ile incelenmesi neticesinde Türkiye için geçerli olabilecek bir matematiksel formül

elde edilmiştir. Bu formül yer hareketi parametreleri ile bu parametreleri etkileyen diğer faktörler arasındaki ilişkiyi sağlamaktadır.

Bu analizin neticesinde pik zemin ivme değerlerinin ve spektral ivme değerlerinin tahmini için elde edilen ifadelerin, Türkiye'nin deprem riski taşıyan bölgelerinde dizayn amaçlı kullanılmak üzere zemine, mesafeye ve magnitude bağlı tepki spektrumunun oluşturulmasında yararlı olacağı görülmüştür. Elde edilen sonuçlar 1997 Uniform Building Code ve Türkiye deprem şartnamesindeki spektral eğriler ile karşılaştırılmış ve Türkiye için geçerli olan dizayn spektrumlarının aktif faylardan 10 km mesafeden sonra yüksek ivme değerleri verdiği görülmüştür. Hesap sonuçlarına göre bu çalışmada verilen tepki spektrum modelleri zemine bağlı yer hareketi dizayn parametrelerinin belirlenmesinde özellikle geniş bir aralık içerisinde magnitud, mesafe ve değişik zemin durumları için daha gerçekçi yaklaşımlar sunmaktadır. Bu anlamda elde edilen sonuçlar senaryo depremleri ve deprem risklerinin azaltılması çalışmalarında etkili bir şekilde kullanılabilirler. Ayrıca yapılan karşılaştırmalar, belirli bir bölge için oluşturulmuş dizayn spektrumlarının başka bir bölgenin hesaplarında direkt olarak kullanılamayacağını göstermiştir.

Anahtar Kelimeler: Azalım ilişkisi, deprem tehlikesi, doğrusal olmayan regresyon analizi, zemine bağımlı tepki spektrumu, kayma dalgası hızı.

To my wife, Narmina...

ACKNOWLEDGMENTS

I would like to express my deepest gratitude to my supervisor Prof. Dr. Polat Gülkan for his patient guidance, careful supervision and helpful suggestions. I am also grateful to Dr. Engin Karaesmen and Assoc.Prof.Dr. Azer Kerimov for the discussion of statistical analysis methods.

I acknowledge with gratitude the help of Sinan Akkar, Altuğ Erberik and Tolga Yılmaz in the Earthquake Engineering Research Center at Middle East Technical University (METU/EERC). Sincere thanks are extended to Zahide Çolakoğlu, Tülay Uğraş and Uluğbey Çeken in General Directorate of Disaster Affairs, Earthquake Research Department for providing references and necessary data.

TABLE OF CONTENTS

ABSTRACT	iii
ÖZ	v
ACKNOWLEDGMENT	viii
TABLE OF CONTENTS	ix
LIST OF TABLES	xi
LIST OF FIGURES	xii
LIST OF SYMBOLS	xviii
CHAPTER	
1. INTRODUCTION	
1.1 General	1
1.2 Object and Scope	2
1.3 Organization and Contents	2
1.4 Strong Motion Network in Turkey	3
2. STRONG MOTION DATABASE	
2.1 General	5
2.2 Moment Magnitude	8
2.3 Distance from Fault	10
2.4 Local Site Geology	12
2.5 Fault Mechanism	17
2.6 Peak Horizontal Acceleration (PHA)	17
2.7 Selection of Attenuation Relationship Model	19
3. DERIVATION OF ATTENUATION RELATIONSHIP	
3.1 General	22
3.2 Attenuation Relationship Development	23
3.3 Model Adequacy Checking	31
3.4 Estimation of σ^2	32

3.5 Comparison with Other Ground Motion Relationships.....	41
3.6 Uncertainty and Reliability	47
4. EARTHQUAKE HAZARD AND SITE-DEPENDENT RESPONSE SPECTRA	
4.1 General	49
4.2 Site Dependent Spectra	49
4.3 Smooth Site-Dependent Response Spectra	55
4.4 Comparison with Regulatory Turkish Spectra	58
4.5 Comparison with UBC 1997 Response Spectra	65
5. SUMMARY, CONCLUSIONS AND RECOMMENDATIONS	
5.1 Summary	68
5.2 Discussion and Conclusions	69
5.3 Future Recommendations	71
REFERENCES	73
APPENDICES	
A. Details of Strong Motion Database	77

LIST OF TABLES

TABLES

2.1	Earthquakes used in the analysis	15
3.1	Attenuation relationships of horizontal PGA and response spectral accelerations (5% damping)	25

LIST OF FIGURES

FIGURES

1.1	The locations of strong motion accelerographs in Turkey	4
2.1	Map of seismic activity of Turkey in the last century	6
2.2	Locations of recording stations used in the database	7
2.3	Relationship between the various magnitude scales	9
2.4	Most commonly used measures of distance	11
2.5	The distribution of recordings in database in terms of magnitude and distance	12
2.6	Histogram of shear wave velocity	15
2.7	The distribution of recordings in database in terms of magnitude, distance and local geological conditions	16
2.8	The distribution of recordings in database in terms of magnitude, distance and faulting mechanism	18
2.9	Distribution of the larger maximum horizontal acceleration of either component versus distance	19

2.10	Comparisons of the North Anatolian Fault and San Andreas Fault	21
3.1	Curves of peak acceleration versus distance for magnitude 5.5, 6.5 and 7.5 earthquakes at rock sites	26
3.2	Curves of peak acceleration versus distance for magnitude 5.5, 6.5 and 7.5 earthquakes at soil sites	27
3.3	Curves of peak acceleration versus distance for magnitude 5.5, 6.5 and 7.5 earthquakes at soft soil sites	27
3.4	Curves of spectral acceleration for 0.3s versus distance for magnitude 5.5, 6.5 and 7.5 earthquakes at rock sites	28
3.5	Curves of spectral acceleration at 0.3s versus distance for magnitude 5.5, 6.5 and 7.5 earthquakes at soil sites	28
3.6	Curves of spectral acceleration at 0.3s versus distance for magnitude 5.5, 6.5 and 7.5 earthquakes at soft soil sites	29
3.7	Curves of spectral acceleration at 1s versus distance for magnitude 5.5, 6.5 and 7.5 earthquakes at rock sites	29
3.8	Curves of spectral acceleration at 1s versus distance for magnitude 5.5, 6.5 and 7.5 earthquakes at soil sites	30
3.9	Curves of spectral acceleration at 1s versus distance for magnitude 5.5, 6.5 and 7.5 earthquakes at soft soil sites	30
3.10	Pseudo velocity response spectra for 7.5-magnitude earthquake at soil sites for distances 0, 10, 20, 40 and 80km	31

3.11	Curves of peak acceleration versus distance for magnitude 7.4 and 6.0 earthquakes at rock sites	33
3.12	Curves of peak acceleration versus distance for magnitude 7.4 earthquake at soil and soft soil sites	34
3.13	Curves of peak acceleration versus distance for magnitude 7.4 earthquake at soft soil site	35
3.14	Curves of spectral acceleration at $T = 0.3s$ versus distance for magnitude 7.4 and 6.0 earthquakes at rock sites	36
3.15	Curves of spectral acceleration at $T = 0.3s$ versus distance for magnitude 7.4 earthquake at soil and soft soil sites	37
3.16	Curves of spectral acceleration at $T = 0.3s$ versus distance for magnitude 6.5 earthquake at soft soil site	38
3.17	Curves of spectral acceleration at $T = 1.0s$ versus distance for magnitude 7.4 and 6.0 earthquakes at rock sites	39
3.18	Curves of spectral acceleration at $T = 1.0s$ versus distance for magnitude 7.4 earthquake at soil and soft soil sites	40
3.19	Curves of spectral acceleration at $T = 1.0s$ versus distance for magnitude 6.5 earthquake at soft soil site	41
3.20	Curves of peak acceleration versus distance for magnitude 7.4 earthquake at rock and soil sites	44
3.21	Curves of spectral acceleration at $T = 0.3 s$ versus distance for a magnitude 7.4 earthquake at rock and soil sites	45

3.22	Curves of spectral acceleration at $T = 1.0$ s versus distance for a magnitude 7.4 earthquake at rock and soil sites	46
3.23	Differences caused by using the larger of the two horizontal components or the component in the direction of the largest resultant	47
4.1	Anticipated mean spectra for magnitude 6.5 earthquake at distance of 5.0 km for various geological conditions	51
4.2	Anticipated mean spectra for magnitude 7.0 earthquake at distance of 5.0 km for various geological conditions	51
4.3	Anticipated mean spectra for magnitude 7.5 earthquake at distance of 5.0 km for various geological conditions	52
4.4	Anticipated mean spectra for magnitude 6.5 earthquake at distance of 10.0 km for various geological conditions	52
4.5	Anticipated mean spectra for magnitude 7.0 earthquake at distance of 10.0 km for various geological conditions	53
4.6	Anticipated mean spectra for magnitude 7.5 earthquake at distance of 10.0 km for various geological conditions	53
4.7	Anticipated mean spectra for magnitude 7.5 earthquake at distance of 10.0 km for various geological conditions	54
4.8	Anticipated mean spectra for magnitude 7.5 earthquake at distance of 10.0 km for various geological conditions	54
4.9	Anticipated mean spectra for magnitude 7.5 earthquake at distance of 10.0 km for various geological conditions	55

4.10	General response spectrum for 5% damping	56
4.11	Smoothed mean spectra (5% damping) for magnitude 7.5 earthquake for various distances at rock sites	57
4.12	Smoothed mean spectra (5% damping) for magnitude 7.5 earthquake for various distances at soil sites	57
4.13	Smoothed mean spectra (5% damping) for magnitude 7.5 earthquake for various distances at soft soil sites	58
4.14	Code basis design acceleration spectrum for 5% damping	59
4.15	Comparison of proposed design spectra for 5 percent of critical damping and computed response spectra for the N-S and E-W components of Dinar, Dinar Earthquake of 1995	61
4.16	Comparison of proposed design spectra for 5 percent of critical damping and computed response spectra for the E-W component of Sakarya, Kocaeli Earthquake of 1999	61
4.17	Comparison of proposed design spectra for 5 percent of critical damping and computed response spectra for the N-S and E-W components of Yarımca, Kocaeli Earthquake of 1999	62
4.18	Comparison of proposed design spectra for 5 percent of critical damping and computed response spectra for the N-S and E-W components of İzmit, Kocaeli Earthquake of 1999	62
4.19	Comparison of proposed design spectra for 5 percent of critical damping and computed response spectra for the N-S and E-W components of Düzce, Kocaeli Earthquake of 1999	63

4.20 Comparison of proposed smooth spectra for 5 percent of critical damping and current seismic code for various geological conditions	64
4.21 Comparison of proposed smooth spectra for 5 percent of critical damping and current seismic code for various geological conditions	64
4.22 Comparison of normalized spectra for 5 percent of critical damping for different site conditions at distances of 2 km	66
4.23 Comparison of normalized spectra for 5 percent of critical damping for different site conditions at distances of 10 km	66
4.24 Comparison of smooth spectra for 5 percent of critical damping for rock soil and soft soil conditions at various distances	67

LIST OF SYMBOLS

a	Acceleration
A	Area of fault surface
A_0	Effective ground acceleration coefficient
$A(T)$	Spectral acceleration coefficient
d	Displacement
D	Average displacement
I	Building importance factor
h	Fictitious depth
M_b	Body wave magnitude
M_L	Richter local magnitude
M_0	Seismic moment
M_S	Surface wave magnitude
M_w	Moment magnitude
R	Response Modification factor
$R_a(T)$	Seismic load reduction factor
R_{cl}	Closest distance
$S(T)$	Spectrum coefficient
T	Undamped natural period of oscillator
T_A	First corner period of smoothed spectra
T_B	Second corner period of smoothed spectra
v	Velocity
V_A	Fictitious shear wave velocity
V_S	Shear wave velocity
Y	Predicted parameter
Z	Seismic zone factor

μ	Shear modulus
σ	Error term
PGA	Peak ground acceleration
PHA	Peak horizontal acceleration
PSA	Peak spectral acceleration

CHAPTER 1

INTRODUCTION

1.1. GENERAL

Earthquakes are one of nature's greatest hazards to life on this planet; throughout historic times they have caused the destruction of countless cities and settlements on nearly every continent. They are the least understood of the natural hazards and in early days were looked upon as supernatural events. Possibly for this reason earthquakes have excited concern, which is out of proportion to their actual hazard.

Ground vibrations during an earthquake can severely damage buildings and equipment housed in them. The ground acceleration, velocity and displacements (referred to as ground motion), when transmitted through a structure, are in most cases amplified. The amplified motion can produce forces and displacements, which may exceed those the structure can sustain. Many factors influence this ground motion and its amplification. An understanding of how these factors influence the response of structures is essential for a safe and economical design.

Prediction of ground shaking expected at each location is therefore fundamental for the calculation of the resulting losses and obtaining reliable designs. Furthermore, with the exception of surface fault rupture and tsunamis, all of the other secondary hazards associated with earthquakes, particularly liquefaction and landslides, are also a direct consequence of the intensity of the ground shaking.

In many years from past to now, many attempts have been made to establish damage predictor parameters for earthquake affecting buildings. The use of quantitative ground motion parameters such as Peak Ground Acceleration (PGA) has become more favorable in recent years, and the current movement is towards the use of response spectra and capacity curves. The new estimation method is carried out on the behavior of the building itself by the use of spectral response ordinates.

In order to apply this technique, to obtain valid earthquake hazard programs and loss functions, firstly it is essential to have a suitable and reliable earthquake attenuation relationship to describe the effects of any anticipated possible earthquakes within the specified boundaries.

1.2. OBJECT AND SCOPE

The primary purpose of this document is to provide comprehensive methodology and supporting commentary for the derivation of attenuation relationship for Turkey by using strong motion data, and ground shaking properties of past earthquakes and then to construct site geology, fault mechanism, and distance dependent response spectra for possible use in design for any earthquake region in Turkey. This dissertation is intended to serve as a reference for the design of critical buildings and future seismic hazard studies.

1.3. ORGANIZATION AND CONTENTS

This thesis is organized into 5 chapters. Chapter 1 is the introductory part describing the seismic shaking and its consequences. Chapter 2 provides detailed information about the strong motion database and predictor parameters required to develop the analytical model and brief information about selection of model attenuation relationship. Chapter 3 presents derivation of estimation equations, detailed results of regression analysis, comparisons with other ground motion relationships and uncertainties within the process of estimation. Chapter 4 provides

detailed discussion of the regression analysis results with their use in developing of site-dependent response spectra and in earthquake hazard studies. In Chapter 5, concluding remarks and discussion, brief summary and future recommendations are presented.

1.4. STRONG GROUND MOTION NETWORK IN TURKEY

Ground motion during an earthquake is measured by a strong motion accelerograph, which records the acceleration of the ground at a particular location. Three orthogonal components of the motion, two in the horizontal direction and one in the vertical are recorded by these instruments. In this study among the three components of each records (one in vertical and two in horizontal directions) vertical component is ignored and analyses are performed on the basis of N-S and E-W components, which are the traditional orientations in Turkey.

The strong motion network in Turkey was initially started in 1973. The strong motion recording instruments are located on free field or mounted inside the structures. Most of these instruments are located in meteorological stations up to three stories tall because the strong motion stations in Turkey are co-located with institutional facilities for ease of access, phone hook-up and security. As of November 2001, there are about 130 strong motion recording stations all around the country. Since the number of instruments is limited, they are located in high earthquake activity zones of Turkey. These high activity zones are the following: North Anatolian Fault zone, East Anatolian Fault zone and Graben zones of West Anatolia. The averaged distance between the instruments is in the order of 50-60 kilometers. This is so that, in case of any destructive earthquake, at least one strong ground motion can be recorded. The locations of strong motion accelerographs in Turkey are illustrated in Figure 1.1 and the list of the used ground motion recording stations for each earthquake data respectively are given in Table A.1 in Appendix A.

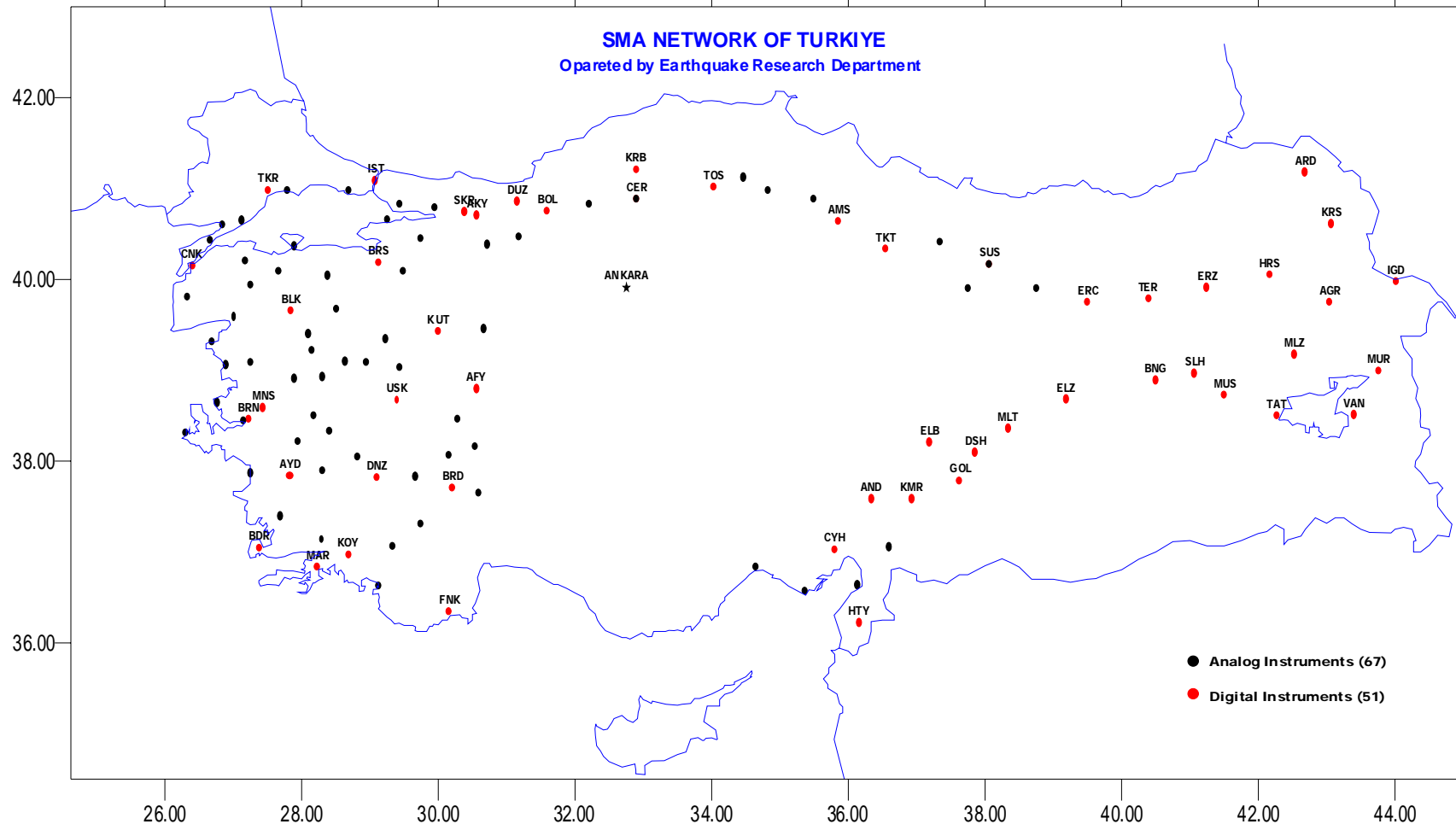


Figure 1.1 Instrument locations for national network

CHAPTER 2

STRONG MOTION DATABASE

2.1. GENERAL

Turkey is one of the active regions in the world as witnessed by the occurrence interval of strong earthquakes. This situation can be best viewed in the map of seismic activity of Turkey in the last century, which is shown in Figure 2.1. In Turkey almost all the earthquakes are shallow earthquakes and these types of earthquakes in active tectonic regions have provided the largest amount of ground motion data and the refine largest number/points in development of attenuation relationships. With this large data set, effects of parameters in attenuation formula can be evaluated more accurately and reliable and appropriate relationships can be developed.

The characteristics of ground motion vary with the nature and the size of the event at the source and with the distance from the source. Traditionally the peak ground motions have been described as a function of earthquake magnitude, closest distance from the source, soil property of the site and lastly faulting type. Detailed discussions of the influences of these parameters are given in the following paragraphs. After carefully searching the strong motion and local geologic database of Turkey, a total of 93 records from 47 horizontal components of 19 events that occurred between 1976-1999 were chosen for the analysis. This strong motion database is presented in Table A.1. The epicenter coordinates of the earthquakes used in the database and locations of the recording stations are illustrated in Figure 2.2.

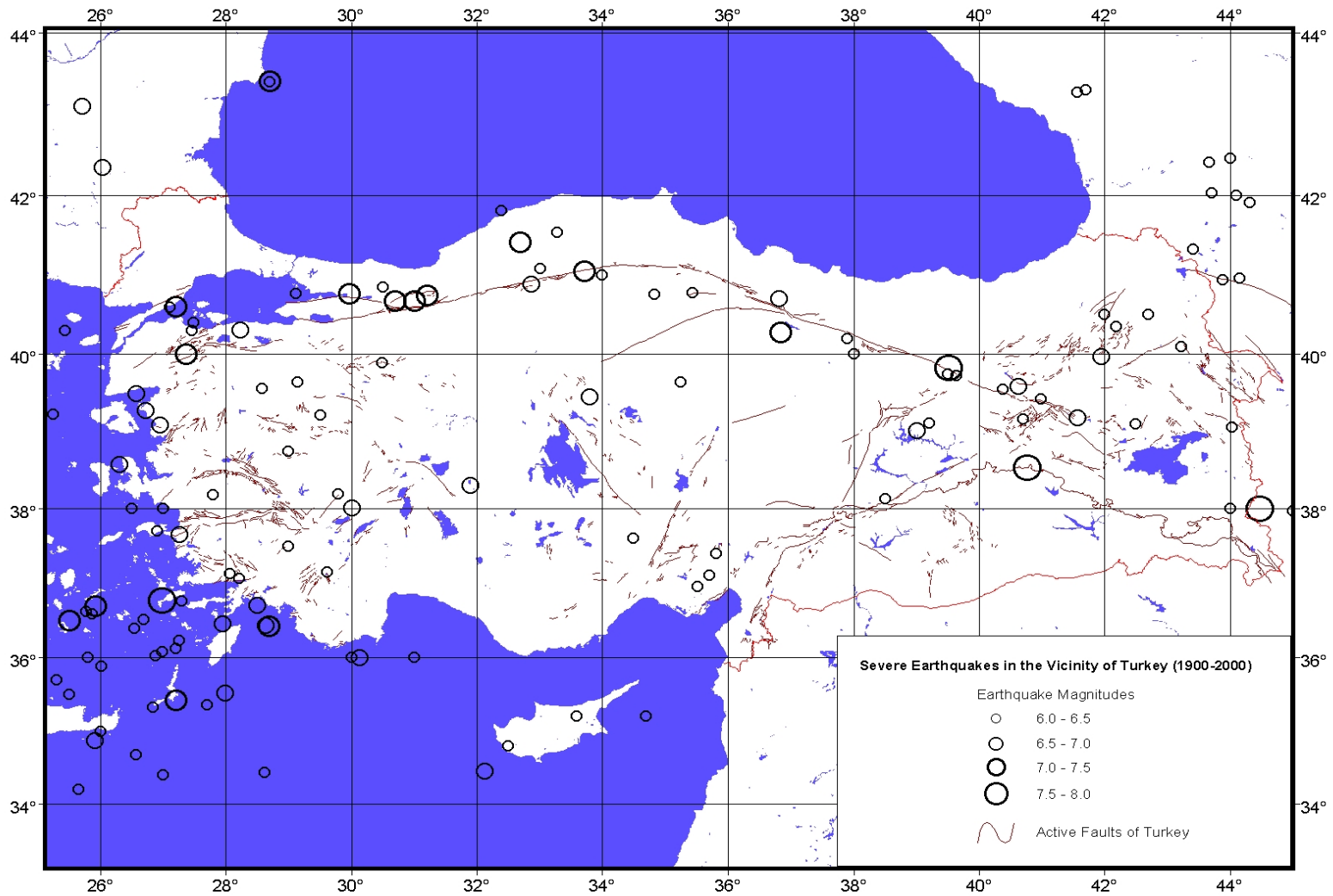


Figure 2.1 Seismic activities during last century

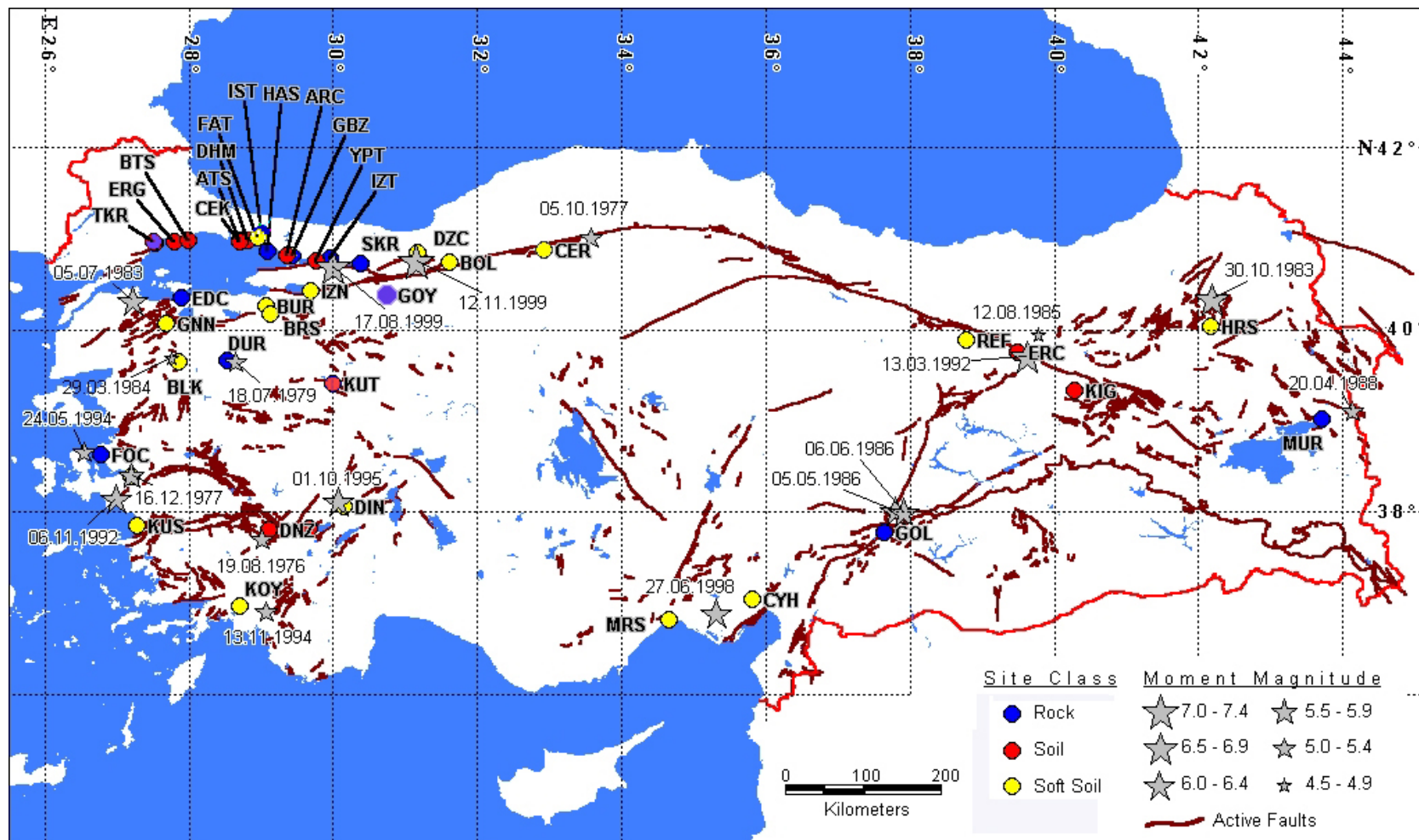


Figure 2.2 Earthquakes used in the analysis with the locations of strong motion recording stations

2.2. MOMENT MAGNITUDE

The possibility of obtaining a more objective, quantitative measure of the size of an earthquake came about with the development of modern instrumentation for measuring ground motion during earthquakes. In the past 60 years, the development of seismic instruments, and our understanding of the quantities and their measure have increased dramatically. Seismic instruments allow an objective, quantitative measurement of earthquake size called earthquake magnitude to be made. Measurements of earthquake magnitude are instrumental (i.e., based on some measured characteristic of ground shaking).

In the determination process, moment magnitude was used among the other scales because it is important that Richter Local Magnitude, Surface Wave Magnitude, Body Wave Magnitude scales are empirical quantities based on various instrumental measurements of ground shaking characteristics (seismic wave amplitudes). However, it is known that as the total amount of energy released during an earthquake increases, the ground shaking characteristics do not necessarily increase at the same rate. For strong earthquakes, the measured ground-shaking characteristics become less sensitive to the size of the earthquake than for smaller earthquakes. This phenomenon is referred to as *saturation*; the body wave, M_b and Richter local magnitudes, M_L saturate at magnitudes of 6 to 7 and the surface wave magnitude, M_S saturates at about $M_S = 8$. To describe the size of very large earthquakes, a magnitude scale that does not depend on ground-shaking levels and consequently does not saturate, would be desirable. The moment magnitude scale (M_w) is the only magnitude scale which does not suffer from the above mentioned saturation problem for great earthquakes. The reason is that it is directly based on the forces that work at the fault rupture to produce the earthquake and not on the recorded amplitude of specific types of seismic waves [1]. The moment magnitude is given by the following formula [2]:

$$M_w = (\log M_0 / 1.5) - 10.7 \quad (2.1)$$

Here: M_0 is the seismic moment in dyne-cm and this quantity of an earthquake is given by [2]:

$$M_0 = \mu A D \quad (2.2)$$

Here: μ is the shear modulus usually taken as 3×10^{11} dyne/cm² for crustal faults, D is the average displacement across the fault surface; and A is the area of the fault surface that ruptured. The seismic moment is named for its units of force times length; however, it is more a measure of the work done by the earthquake. As such, the seismic moment correlates well with the energy released during an earthquake. Further, the seismic moment can be estimated from geologic records of historical earthquakes [2].

The relationships between the various magnitude scales are given in Figure 2.3. In this figure, saturations of the instrumental scales are indicated by their flat parts at higher magnitudes [3].

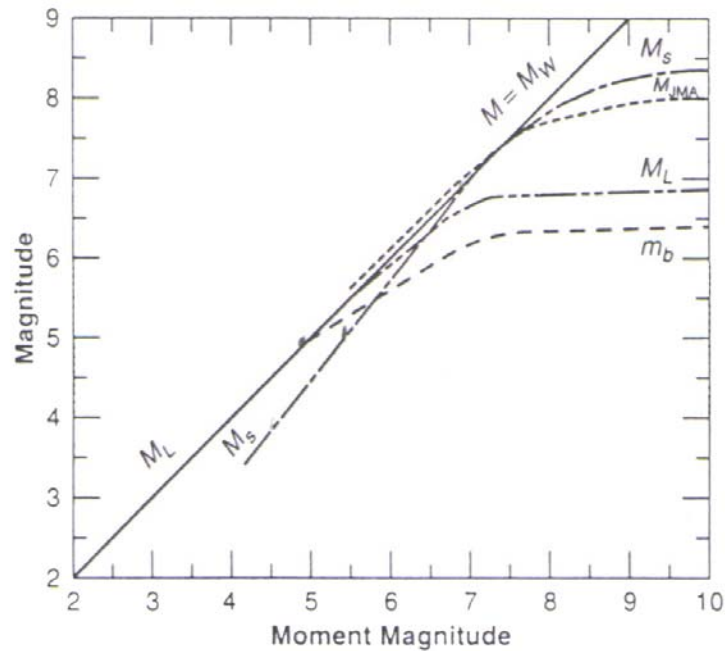


Figure 2.3 Relationship between the various magnitude scales [3]

In the database, some of the old earthquake records have no information related to their moment magnitudes or calculated seismic moments; they have only M_S , M_L or M_b values. Because of this reason the magnitude scales were converted to moment magnitude according to the relations listed in Wells and Coppersmith (1994) and by using transformations curves given in Figure 2.3. The final moment magnitude values used in the regression analysis for each earthquake are listed in Table A.1.

The magnitudes are restricted to about $M_w \geq 5.0$ to emphasize those ground motions having greatest engineering interests, and to limit the analysis to the more reliably recorded events. In the regression phase, magnitudes of earthquakes were locked within ± 0.25 band intervals centered at halves or full numbers in order to eliminate the errors coming from the determination of these magnitude values.

2.3. DISTANCE FROM FAULT

Much of the energy released by rupture along a fault takes the form of stress waves. Since the amount of energy released in an earthquake is strongly related to its magnitude, the characteristics of the stress waves will also be strongly related to magnitude.

As stress waves travel away from the source of an earthquake, they spread out and are partially absorbed by materials they travel through. As a result, the *specific energy* (energy per unit volume) decreases with increasing distance from the source. Since the characteristics of stress waves are strongly related to specific energy, they will also be strongly related to distance. The distance between the source of an earthquake and a particular site can be interpreted in different ways. Figure 2.4 illustrates some of the most commonly used measure of distances. R_1 and R_2 are hypocentral and epicentral distances, which are the easiest distances to determine after an earthquake. The length of fault rupture is a significant fraction of the distance between the fault and the site, however, energy may be released closer to the site, and R_1 and R_2 may not accurately represent the effective distance. R_3 is the

distance to the zone of highest energy release. Since rupture of this zone is likely to produce the peak ground motion amplitudes, it represents the best distance measure for peak amplitude predictive relationships. Unfortunately, its location is difficult to determine after an earthquake. R4 is the closest distance to the zone of rupture (not including sediments overlying basement rock) and R5 is the closest distance to the surface projection of the fault rupture. R4 and R5 have both been used extensively in predictive relationships [3].

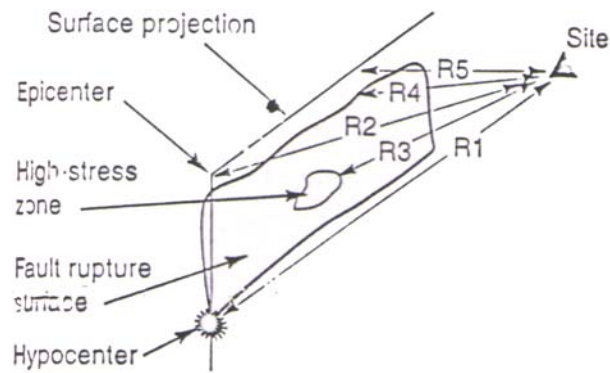


Figure 2.4. Most commonly used measures of distance

In this study, distance is defined as the closest horizontal distance between the recording station and a point on the horizontal projection of the rupture zone on the earth's surface (r_{cl}) (R5 in Figure 2.4). However, for some of the smaller events, rupture surfaces have not been defined clearly therefore epicentral distances are used instead of closest distance. It is believed that using epicentral distance does not introduce significant bias because the dimensions of rupture for small earthquakes are usually much smaller than the distance to the recording stations. The closest distance values used for all earthquake records are given in Table A.1 and the graphical representation of closest distance versus moment magnitude is shown in Figure 2.5. Recordings from small earthquakes were limited to the closer distances than large earthquakes depending on the magnitude and the geology of the recording site to minimize the influence of regional differences in attenuation and to avoid the complex propagation effects coming from longer distances.

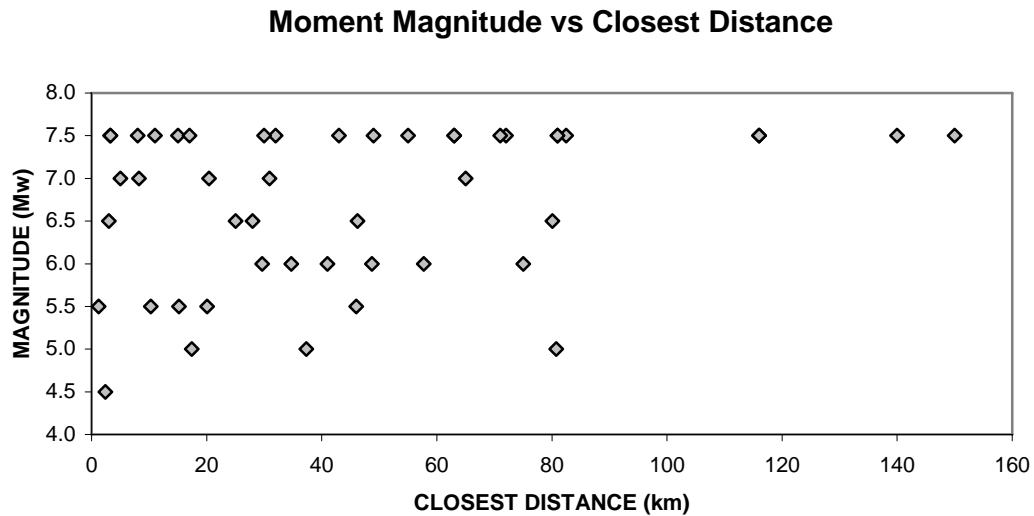


Figure 2.5 Distribution of recordings in database in terms of magnitude and distance

2.4. LOCAL SITE GEOLOGY

Local geology and soil conditions of the site will determine the characteristics of earthquake ground motions that may be experienced and its attenuation. Based on the investigation of the local geology and composition of soils in the area, it is possible to anticipate what type of motions will occur at the site in terms of frequency, acceleration, velocity and amplitude for given earthquakes.

Local soil conditions at a specific site also have a significant effect on ground-shaking amplitudes. Basic rock motions have certain characteristics associated with sharp, high frequency accelerations and velocity movements. As seismic waves travel through less dense soils, motions are modified by the depth of soil overburden, which increases the amplitude of motion and emphasizes the longer, dominant periods of vibration.

Studies of the 17 August 1999 Kocaeli and the 12 November 1999 Düzce earthquakes indicated that the most damaging motions occur in zones of deeper, less

consolidated soils, in contrast to bedrock sites [5]. In several other earthquakes, many severe building damages have been identified in areas where deep alluvium soils were located over bedrock.

Correlations between structural damage and the depth to rock at sites with similar soil conditions have shown that high-rise buildings with low natural frequencies have sustained the greatest damage when sited on deep soil deposits. However shorter and stiffer buildings with higher natural frequencies have been most vulnerable when sited on shallower deposits or on rock. This indicates that the depth to rock affects the frequency content of the seismic waves transmitted to the ground surface. Local site conditions influence the shape of the response spectra and relationships among ground motion parameters (v/a , ad/v^2 where a , v , d are the peak acceleration, velocity and displacement of the ground, respectively).

Effective modulus of soil materials decrease and material damping increases with increasing soil strain levels. Because of these strain-dependent material properties, the amplitudes and frequency content of surface ground motions have been correlated with the strength of the subsurface input motions. Moreover, an increase in the amplitudes of the input motions causes a reduced characteristic frequency of the ground surface motions and a reduced amplification of the input motion as they are transmitted through the overlying soil layers.

Another set of factors is related to the degree of inclination of the layers or the presence of significant topographic features that can greatly influence reflection and refraction processes and the complexity of waves transmitted to the ground surface. For instance, if the soil layers are sharply inclined, horizontal ground motions can no longer be attributed solely to vertically propagating S waves but instead they arise from complex interactions of P waves, S waves and secondary waves [2].

A common trend of studying these effects of geological conditions on ground motion and response spectra is to classify the recording stations according to their

shear-wave velocities. In most of the reliable attenuation relationships, site classes are defined on the basis of the average shear wave velocity in the upper 30m. However, the actual shear-wave velocity and detailed site description are not available for most stations in Turkey. For this reason, the site classifications were estimated by analogy with information in similar geologic materials. The type of geologic materials underlying each recording site was obtained in a number of ways: consultation with geologists in the Earthquake Research Division of Ministry of Public Works and Settlement, various geologic maps, numerous past earthquake reports and geological references prepared for Turkey. On the light of this information soil classes were divided for Turkey into three broad groups: soft soil, soil, and rock. The designated average shear-wave velocities for these groups are 200m/s, 400m/s and 700m/s, respectively. The accepted soil profiles for each station in the database are presented in Table A.1. The histograms of shear-wave velocity of total number of 47 earthquake events used in analysis are given in Figure 2.6 and listing of these earthquakes and the number of recordings for each of the strong motion parameters are listed in Table 2.1. Also the distributions of these events in terms of magnitude, source to the site distance and local geological conditions are given in Figure 2.7. Even if the actual average shear- wave velocities for individual stations are different from the assumed values, the effect on the eventual prediction should not be too drastic.

Table 2.1 Earthquakes used in the analysis

Date	Earthquake	Fault Type	M _w	Number of Recordings		
				Soft Soil	Soil	Rock
19.08.1976	DENİZLİ	Normal	5.3		2	
05.10.1977	ÇERKEŞ	Strike-Slip	5.4	2		
16.12.1977	İZMİR	Normal	5.5	2		
18.07.1979	DURSUNBEY	Strike-Slip	5.3			2
05.07.1983	BİGA	Reverse	6.0	2		4
30.10.1983	HORASAN-NARMAN	Strike-Slip	6.5	2		
29.03.1984	BALIKESİR	Strike-Slip	4.5	2		
12.08.1985	KİĞİ	Strike-Slip	4.9		2	
05.05.1986	MALATYA	Strike-Slip	6.0			2
06.06.1986	SÜRGÜ (MALATYA)	Strike-Slip	6.0			2
20.04.1988	MURADIYE	Strike-Slip	5.0			2
13.03.1992	ERZİNCAN	Strike-Slip	6.9	2	2	
06.11.1992	İZMİR	Normal	6.1	2		
24.05.1994	GİRİT	Normal	5.4			2
13.11.1994	KÖYCEĞİZ	Normal	5.2	2		
01.10.1995	DİNAR	Normal	6.4	2	2	
27.06.1998	ADANA-CEYHAN	Strike-Slip	6.3	4		
17.08.1999	KOCAELİ	Strike-Slip	7.4	12	16	15
12.11.1999	DÜZCE	Strike-Slip	7.1	6		
Total:				40	24	29

Histogram of Shear Wave Velocity

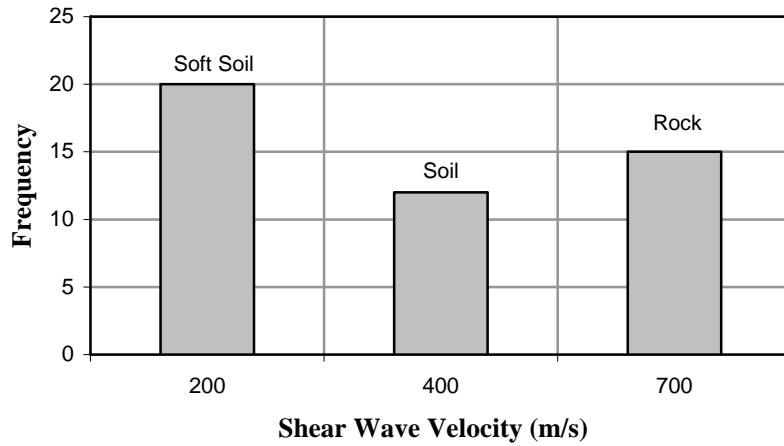


Figure 2.6 Histogram of shear-wave velocity

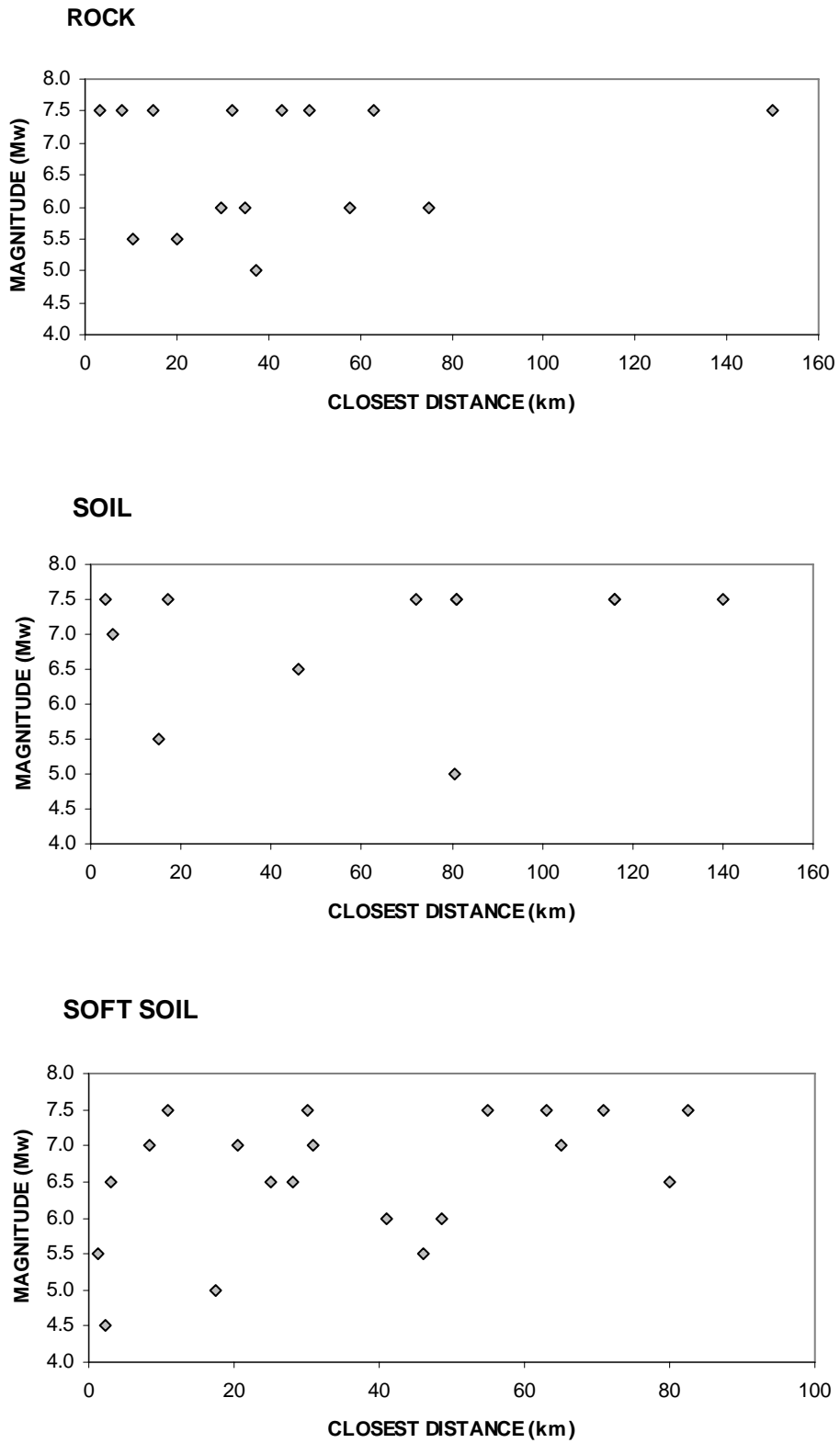


Figure 2.7 Recordings in terms of magnitude, distance and geological conditions

2.5. FAULT MECHANISM

Most of the active faults in Turkey show strike-slip movements and examination of the peak ground motion data from the small number of normal-faulting and reverse faulting earthquakes in the data set showed that they were not significantly different from ground motion characteristics of strike slip earthquakes. For that reason, normal, reverse and strike-slip earthquakes were combined into one single faulting category. The distributions of the used earthquakes in terms of magnitude, source to the site distance and faulting mechanism are given in Figure 2.8.

2.6. PEAK HORIZONTAL ACCELERATION (PHA)

The most commonly used measure of the amplitude of a particular ground motion is the peak horizontal acceleration (PHA). The PHA for a given component of motion is simply the largest (absolute) value of horizontal acceleration obtained from the accelerogram of that component.

Horizontal accelerations have commonly been used to describe ground motions because of their natural relationship to inertial forces. Indeed, the largest dynamic forces induced in certain types of structures (i.e., very stiff structures) are closely related to the PHA.

In this study, peak acceleration values are taken directly from accelerograms, rather than the processed or instrument-corrected values. This is done to avoid bias in the peak values from the sparsely sampled older data. This bias is not a significant problem with more densely sampled recent data. Total of 93 peak horizontal acceleration values are given in Table A.1, and in this data set maximum values among the N-S and E-W components were selected, which correspond to total of 47 acceleration values.

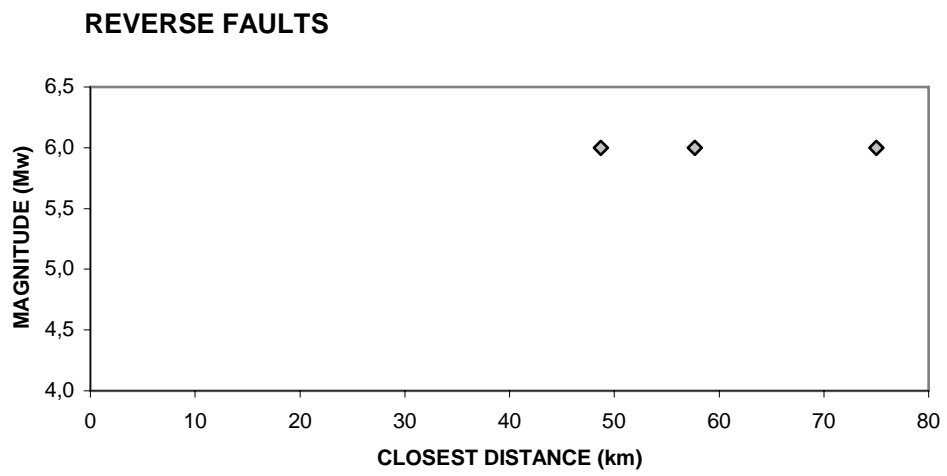
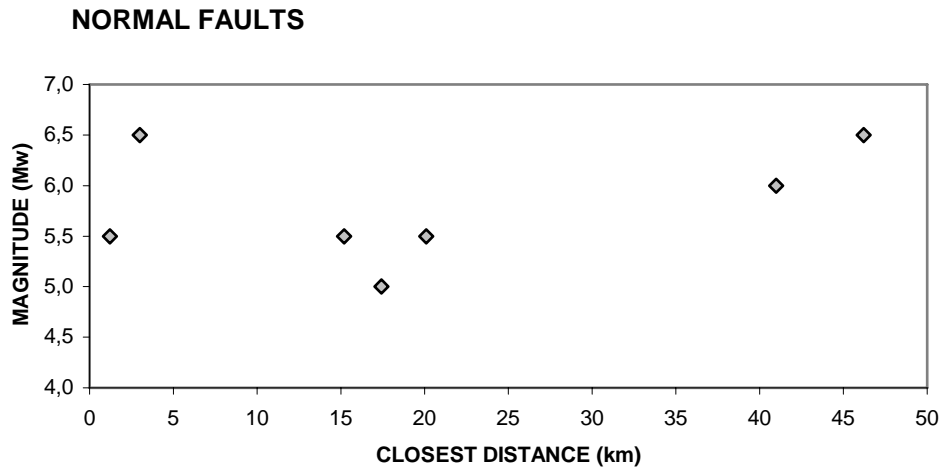
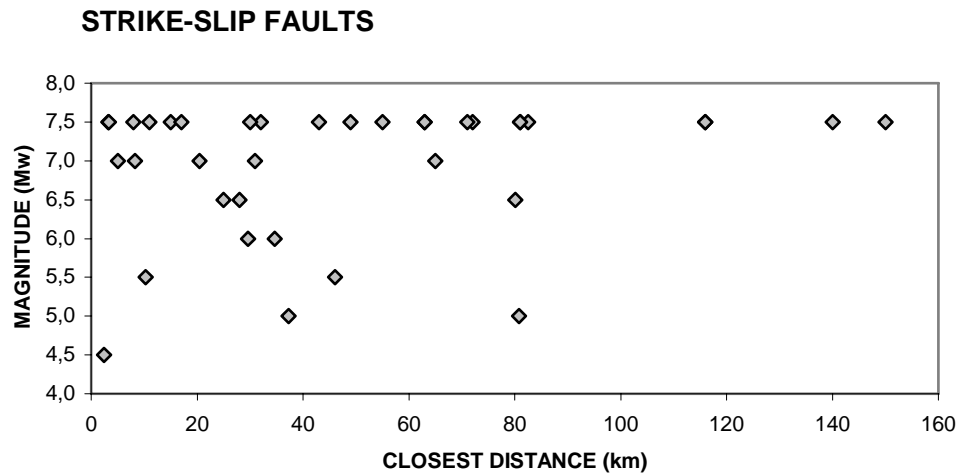


Figure 2.8 Distribution of recordings in database in terms of magnitude, distance and faulting mechanism

The data used in the analysis constitutes only main shocks of 19 earthquakes. They were recorded mostly in small buildings built as meteorological stations. This causes modified acceleration records, as previous analyses have indicated that embedded and large structures can have acceleration values less than those of free-field stations (e.g., Campbell, 1987, 1989a,b). This is one of the unavoidable causes of uncertainties in this study, but there are other attributes that must be mentioned. The first is omission of aftershock data. Most of these come from the two major 1999 events, and contain free-field data that it was not desired to commingle with the rest of the set. Few records for which the peak acceleration caused by the main shock is less than about 0.04 g were omitted. Entire non-discriminated ensemble is shown in Figure 2.9.

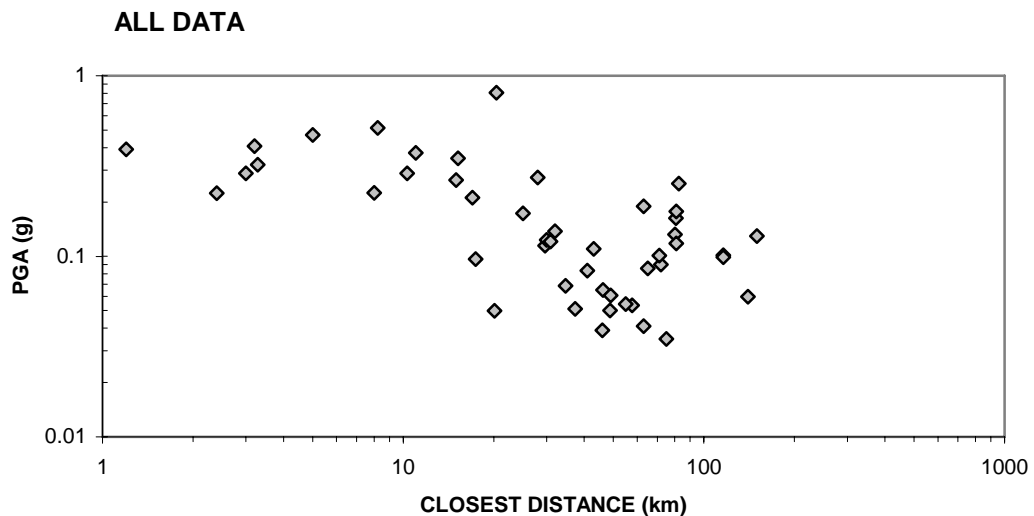


Figure 2.9 Distribution of the larger maximum horizontal acceleration of either component versus distance

2.7. SELECTION OF ATTENUATION RELATIONSHIP MODEL

Predictive earthquake relationships for parameters that decrease with increasing distance (such as peak acceleration and peak velocity) are referred to as attenuation relationships. This relationship is a mathematical formula, derived by regression analysis on real earthquake recordings, relating a particular ground-

motion parameter to the different factors that influence the value of this parameter. Attenuation relationships always include as predictor variables, earthquake magnitude and distance from the source to the site. Most attenuation relationships, especially those for response spectral ordinates also include the effect of surface geology at the site and the mechanism of the fault rupture.

For some parameters, and particularly for PGA, there are many published attenuation equations from which to select for any particular application. There are no attenuation equations published in the international scientific literature that are based on solely Turkish strong-motion data. For this reason it is necessary to have such relationships for Turkey for future seismic hazard mitigation studies.

In the selection of suitable attenuation relationship for Turkey the fault characteristics of North Anatolian Fault and California's San Andreas Fault are taken in to considerations. The 900 km-long North Anatolian Fault has many characteristics similar to California's San Andreas Fault. These two faults are right lateral, strike-slip faults having similar lengths and similar long-term rates of movement. The image given in Figure 2.10 shows comparison between the North Anatolian, Turkey and the San Andreas, California Faults [9]. These geological and geo-tectonic similarities between Anatolia and California (major strike-slip faults similar to North and East Anatolian Faults) and between the Basin and Range regions of Nevada and the Aegean Sea (areas of tectonic extension), and also on the basis of favorable predictive comparisons suggest that it is rational and prudent to take the same form of attenuation relationship currently being used for the assessment of earthquake hazard of Western US, and derive a new estimation equations for Turkey by using this formula.

On the light of this collected information, the relationship model for Turkey is selected from attenuation relationship previously developed by Boore et al. (1997) for shallow earthquakes in Western North America. This selected model is applied to

Turkey by using the strong motion records taken from previous earthquakes occurred in Turkey.

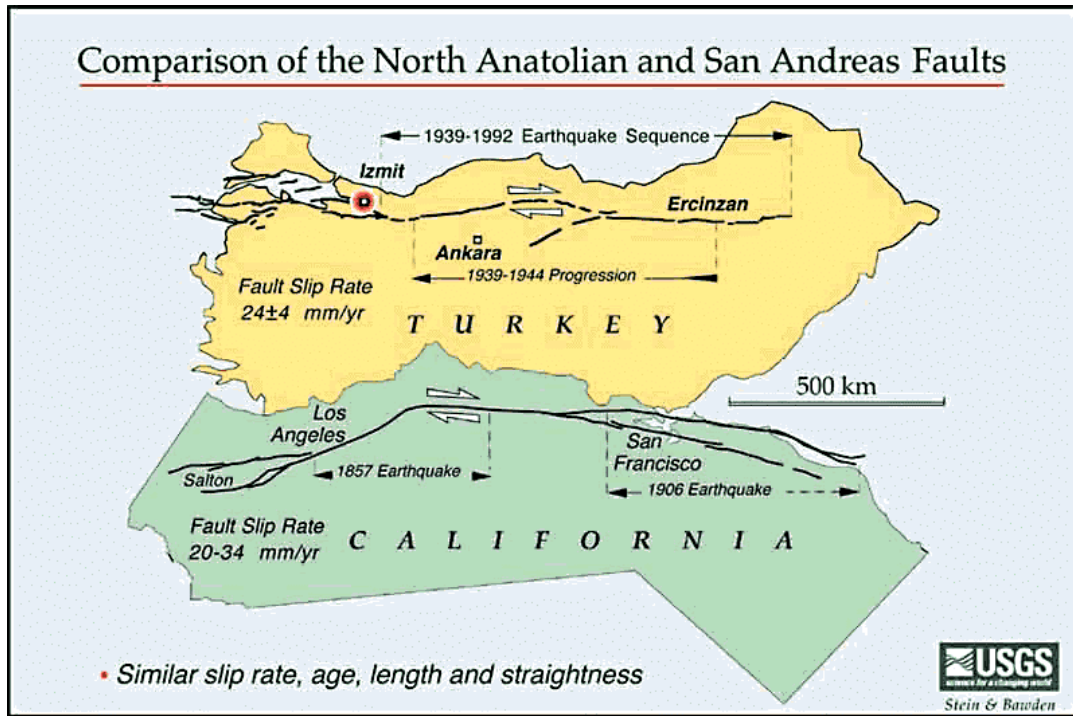


Figure 2.10 Comparisons of the North Anatolian Fault and San Andreas Fault [9]

CHAPTER 3

DERIVATION OF ATTENUATION RELATIONSHIP

3.1. GENERAL

The most obvious piece of information to be gained from an earthquake record is the ground acceleration. In order to estimate the value of this acceleration empirical equations are commonly used and these empirical equations for predicting strong ground motion were typically fit to the strong motion data set by applying regression analysis.

The term regression analysis describes a collection of statistical techniques that serve as a basic for drawing inferences about relationships among quantities in a scientific system. In statistics, numerous regression models exist for evaluating the relationship between any pair of variables, including models for linear or nonlinear relationships and normal (Gaussian) or non-parametric distributions of data. In this study, the coefficients in the equations for predicting ground motion were determined by using nonlinear regression analysis procedure. Nonlinear regression is a method of finding a nonlinear model of the relationship between the dependent variable and a set of independent variables. Unlike traditional linear regression, which is restricted to estimating linear models, nonlinear regression can estimate models with arbitrary relationships between independent and dependent variables. When applying regression analysis those parameters should be quantitative in the data set.

Among the two nonlinear iterative algorithms for estimating the parameters of models that are not linear in the parameters: a sequential quadratic programming algorithm which is more general, suitable for both constrained and unconstrained

problems and a Levenberg-Marquardt algorithm which is generally effective for unconstrained problems are investigated with details. In this study the second algorithm was found more suitable for given cases and selected as a nonlinear regression analysis procedure [11].

This type of nonlinear regression analysis is accomplished using iterative estimation algorithms. The nonlinear regression procedure on the database was performed using SPSS statistical analysis software (Ver.9.00, 1998). This exercise was performed separately on PGA and on peak spectral acceleration (PSA) data at each oscillator period considered (total of 46 periods from 0.1 to 2.0s.).

In this chapter development of attenuation relationship, comparison with other recent estimating equations and reliability of obtained results are presented and discussed in detail.

3.2. ATTENUATION RELATIONSHIP DEVELOPMENT

Attenuation relationships were developed by using the same general form of the equation proposed by Boore et al. (1997). The ground motion parameter estimation equation is as follows:

$$\ln(Y) = b_1 + b_2(M - 6) + b_3(M - 6)^2 + b_5 \ln r + b_V (\ln V_S / V_A) \quad (3.1)$$

$$r = (r_{cl}^2 + h^2)^{1/2} \quad (3.2)$$

Here Y is the ground motion parameter (peak horizontal acceleration (PGA) or pseudo spectral acceleration (PSA) in g.); M is moment magnitude; r_{cl} is closest horizontal distance from the station to a site of interest in km; V_S is shear wave velocity in m/sec. b_1 , b_2 , b_3 , b_5 , h , b_V , and V_A are the parameters to be determined in this equation. Here h is a fictitious depth and V_A is a fictitious shear wave velocity, determined by the regression.

The procedure that we have used to develop the attenuation curves consists of two stages (Joyner and Boore, 1993). In the first, attenuation relationships were developed for PGA and spectral acceleration values by selecting those values in the database as maximum horizontal components of each recording station. Then, a nonlinear regression analysis was performed. In the next stage, random horizontal components were selected for the acceleration values in the database and regression analyses were applied again. The results were compared for PGA, 0.3 s and 1.0 s PSA cases, and it was concluded that selection of maximum, rather than of random, horizontal components did not yield improved estimates and smaller error terms. This issue is taken up again in the section on comparisons of our results with other relations.

The coefficients for estimating the maximum horizontal-component pseudo-acceleration response by Equation (3.1) are given in Table 3.1. The resulting parameters can be used to produce attenuation relationships that predict response spectra over the full range of magnitudes (M_w 5 to 7.5) and distances (r_{cl}) up to 150 km. The attenuation relationship derived in this study shows an expected trend as the shear wave velocity decreases, soil amplitudes become larger than rock. The results were also used to compute errors for PGA and PSA at individual periods. The standard deviation of the residuals, σ , expressing the random variability of ground motions, is an important input parameter in probabilistic hazard analysis. In this study, the observed value of $\ln \sigma$ lies generally within the range of 0.5 to 0.7. The list of standard deviation for each oscillator periods is given in Table 3.1. The calculated attenuation relationships for rock, soil and soft soil sites for PGA, PSA at 0.3s and 1.0s are given in Figure 3.1 through 3.9.

The regression analysis for response spectra was also done on pseudo-velocity response, which is computed by multiplying the relative displacement response by the factor $2\pi/T$, where T is the undamped natural period of oscillator. The curves of pseudo-velocity response spectra for the maximum horizontal component at 5 percent damping for a (M_w) 7.5 earthquake at a soil site for 0, 10, 20, 40 and 80 km are given in Figure 3.10.

Table 3.1 Attenuation relationships of horizontal PGA and response spectral accelerations (5% damping)

$\ln(Y) = b_1 + b_2 (M - 6) + b_3 (M - 6)^2 + b_5 \ln r + b_v (\ln V_S / V_A)$, where $r = (r_c^2 + h^2)^{1/2}$								
Period	b1	b2	b3	b5	b _v	V _A	h	σ _{INY}
PGA	-0.682	0.253	0.036	-0.562	-0.297	1381	4.48	0.562
0.10	-0.139	0.200	-0.003	-0.553	-0.167	1063	3.76	0.621
0.11	0.031	0.235	-0.007	-0.573	-0.181	1413	3.89	0.618
0.12	0.123	0.228	-0.031	-0.586	-0.208	1501	4.72	0.615
0.13	0.138	0.216	-0.007	-0.590	-0.237	1591	5.46	0.634
0.14	0.100	0.186	0.014	-0.585	-0.249	1833	4.98	0.635
0.15	0.090	0.210	-0.013	-0.549	-0.196	1810	2.77	0.620
0.16	-0.128	0.214	0.007	-0.519	-0.224	2193	1.32	0.627
0.17	-0.107	0.187	0.037	-0.535	-0.243	2433	1.67	0.621
0.18	0.045	0.168	0.043	-0.556	-0.256	2041	2.44	0.599
0.19	0.053	0.180	0.063	-0.570	-0.288	2086	2.97	0.601
0.20	0.127	0.192	0.065	-0.597	-0.303	2238	3.48	0.611
0.22	-0.081	0.214	0.006	-0.532	-0.319	2198	1.98	0.584
0.24	-0.167	0.265	-0.035	-0.531	-0.382	2198	2.55	0.569
0.26	-0.129	0.345	-0.039	-0.552	-0.395	2160	3.45	0.549
0.28	0.140	0.428	-0.096	-0.616	-0.369	2179	4.95	0.530
0.30	0.296	0.471	-0.140	-0.642	-0.346	2149	6.11	0.540
0.32	0.454	0.476	-0.168	-0.653	-0.290	2144	7.38	0.555
0.34	0.422	0.471	-0.152	-0.651	-0.300	2083	8.30	0.562
0.36	0.554	0.509	-0.114	-0.692	-0.287	2043	9.18	0.563
0.38	0.254	0.499	-0.105	-0.645	-0.341	2009	9.92	0.562
0.40	0.231	0.497	-0.105	-0.647	-0.333	1968	9.92	0.604
0.42	0.120	0.518	-0.135	-0.612	-0.313	1905	9.09	0.634
0.44	0.035	0.544	-0.142	-0.583	-0.286	1899	9.25	0.627
0.46	-0.077	0.580	-0.147	-0.563	-0.285	1863	8.98	0.642
0.48	-0.154	0.611	-0.154	-0.552	-0.293	1801	8.96	0.653
0.50	-0.078	0.638	-0.161	-0.565	-0.259	1768	9.06	0.679
0.55	-0.169	0.707	-0.179	-0.539	-0.216	1724	8.29	0.710
0.60	-0.387	0.698	-0.187	-0.506	-0.259	1629	8.24	0.707
0.65	-0.583	0.689	-0.159	-0.500	-0.304	1607	7.64	0.736
0.70	-0.681	0.698	-0.143	-0.517	-0.360	1530	7.76	0.743
0.75	-0.717	0.730	-0.143	-0.516	-0.331	1492	7.12	0.740
0.80	-0.763	0.757	-0.113	-0.525	-0.302	1491	6.98	0.742
0.85	-0.778	0.810	-0.123	-0.529	-0.283	1438	6.57	0.758
0.90	-0.837	0.856	-0.130	-0.512	-0.252	1446	7.25	0.754
0.95	-0.957	0.870	-0.127	-0.472	-0.163	1384	7.24	0.752
1.00	-1.112	0.904	-0.169	-0.443	-0.200	1391	6.63	0.756
1.10	-1.459	0.898	-0.147	-0.414	-0.252	1380	6.21	0.792
1.20	-1.437	0.962	-0.156	-0.463	-0.267	1415	7.17	0.802
1.30	-1.321	1.000	-0.147	-0.517	-0.219	1429	7.66	0.796
1.40	-1.212	1.000	-0.088	-0.584	-0.178	1454	9.10	0.790

Table 3.1 Continued

Period	b1	b2	b3	b5	b _v	V _A	h	σ_{INY}
1.50	-1.340	0.997	-0.055	-0.582	-0.165	1490	9.86	0.788
1.60	-1.353	0.999	-0.056	-0.590	-0.135	1513	9.94	0.787
1.70	-1.420	0.996	-0.052	-0.582	-0.097	1569	9.55	0.789
1.80	-1.465	0.995	-0.053	-0.581	-0.058	1653	9.35	0.827
1.90	-1.500	0.999	-0.051	-0.592	-0.047	1707	9.49	0.864
2.00	-1.452	1.020	-0.079	-0.612	-0.019	1787	9.78	0.895

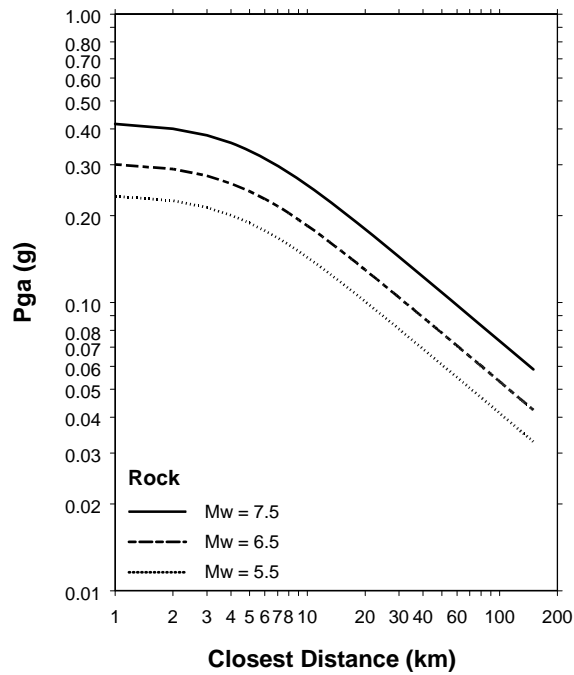


Figure 3.1 Curves of peak acceleration versus distance for magnitude 5.5, 6.5 and 7.5 earthquakes at rock sites

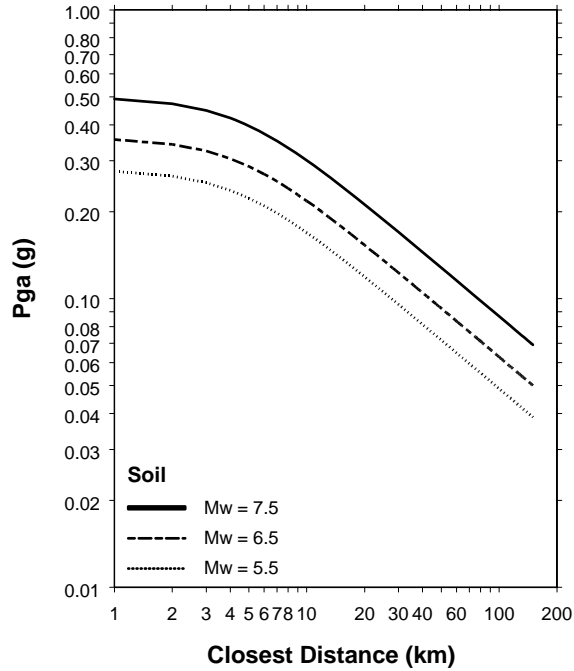


Figure 3.2 Curves of peak acceleration versus distance for magnitude 5.5, 6.5 and 7.5 earthquakes at soil sites

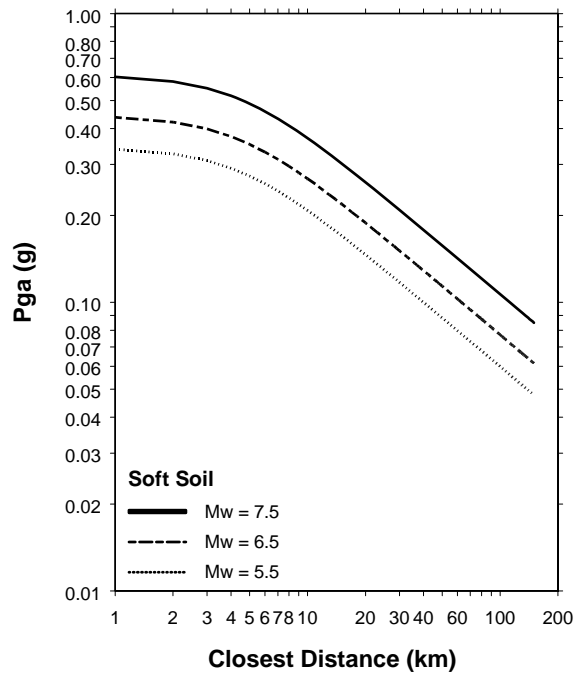


Figure 3.3 Curves of peak acceleration versus distance for magnitude 5.5, 6.5 and 7.5 earthquakes at soft soil sites

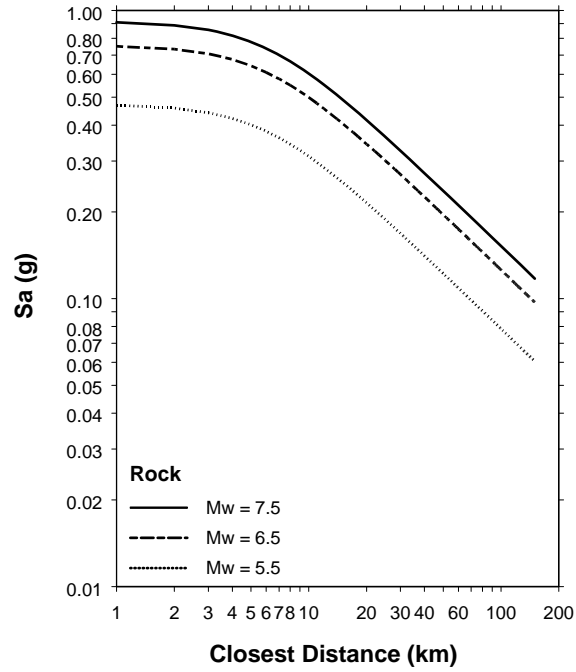


Figure 3.4 Curves of spectral acceleration for 0.3s versus distance for magnitude 5.5, 6.5 and 7.5 earthquakes at rock sites

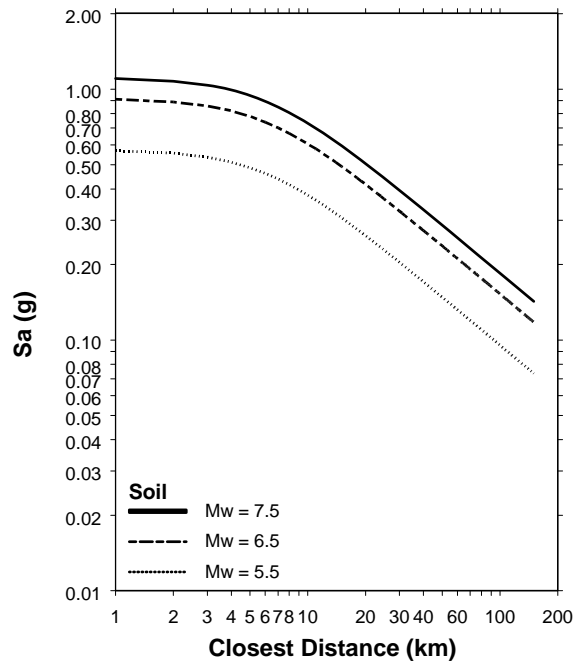


Figure 3.5 Curves of spectral acceleration at 0.3s versus distance for magnitude 5.5, 6.5 and 7.5 earthquakes at soil sites

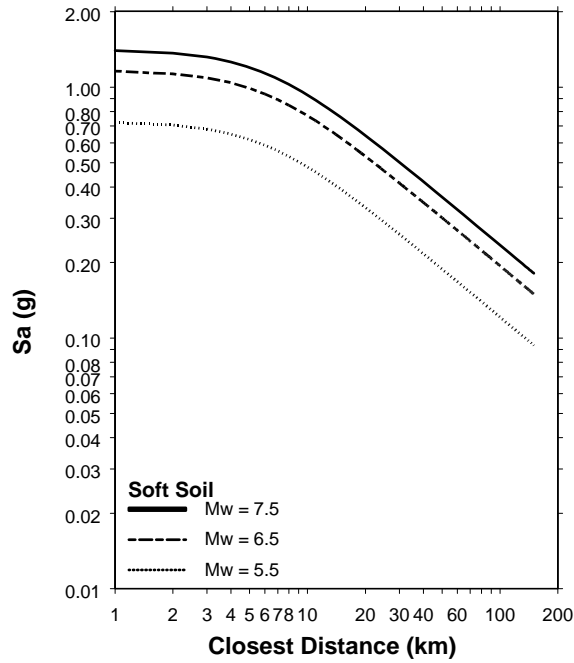


Figure 3.6 Curves of spectral acceleration at 0.3s versus distance for magnitude 5.5, 6.5 and 7.5 earthquakes at soft soil sites

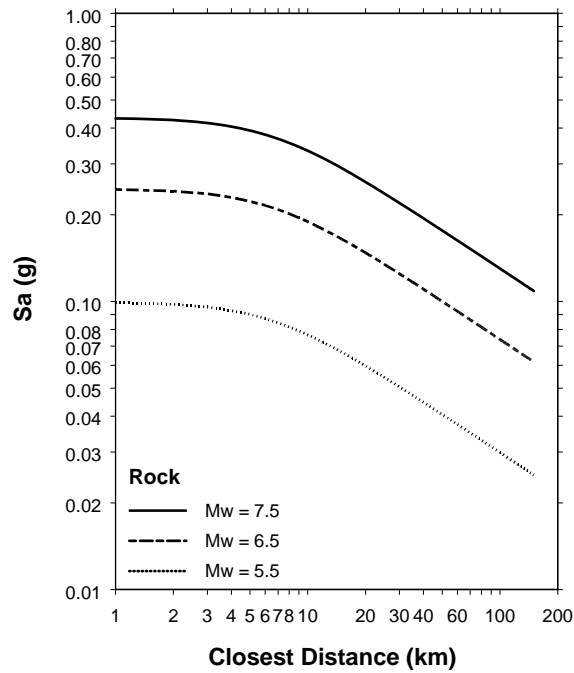


Figure 3.7 Curves of spectral acceleration at 1s versus distance for magnitude 5.5, 6.5 and 7.5 earthquakes at rock sites

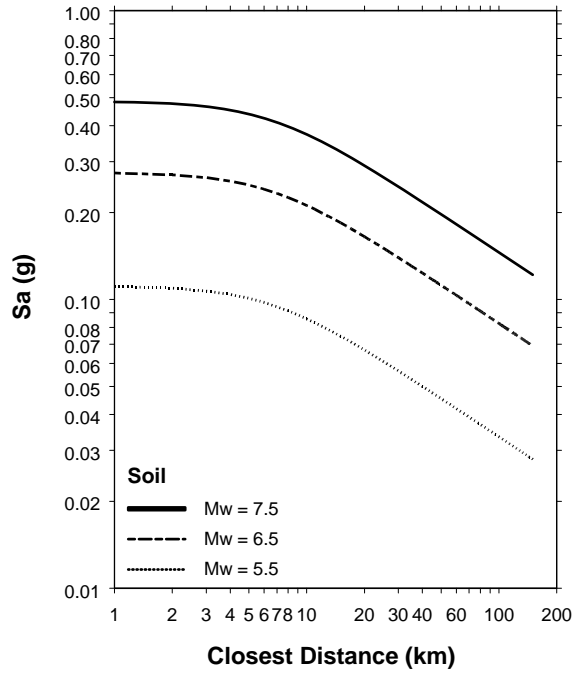


Figure 3.8 Curves of spectral acceleration at 1s versus distance for magnitude 5.5, 6.5 and 7.5 earthquakes at soil sites

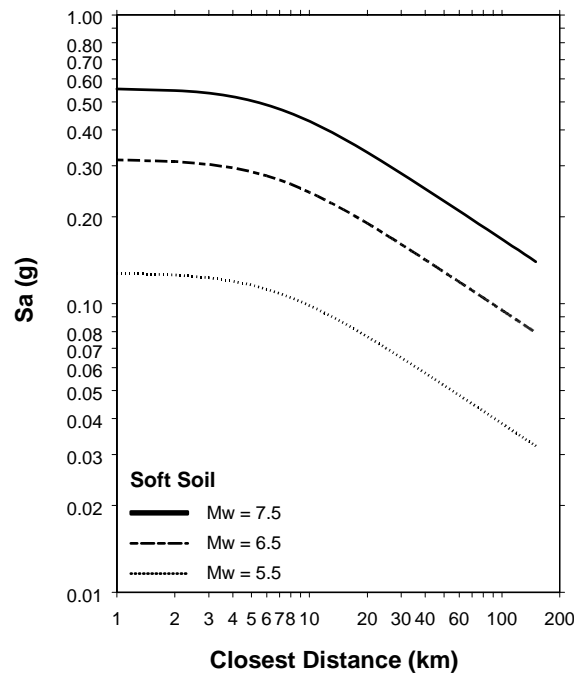


Figure 3.9 Curves of spectral acceleration at 1s versus distance for magnitude 5.5, 6.5 and 7.5 earthquakes at soft soil sites

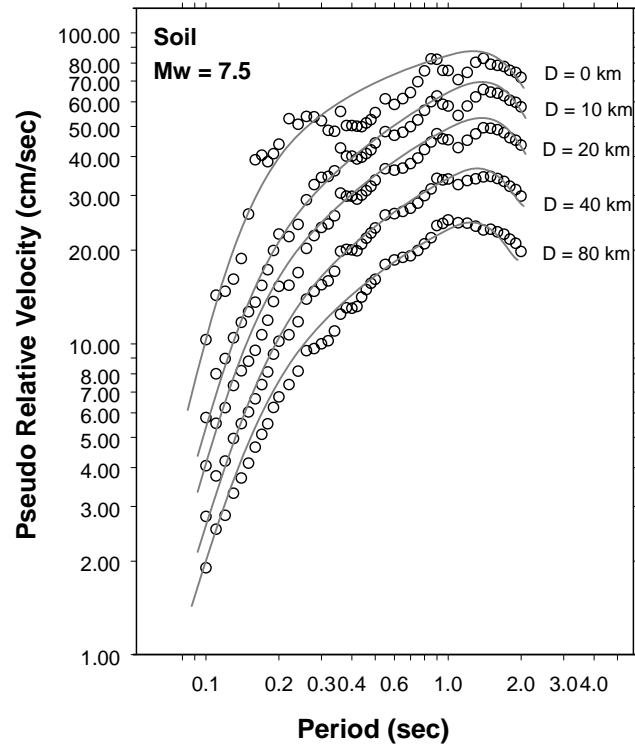


Figure 3.10 Pseudo velocity response spectra for M_w 7.5 earthquake at soil sites for distances 0, 10, 20, 40 and 80 km

3.3. MODEL ADEQUACY CHECKING

The quantity, coefficient of determination (R^2) is used for checking of analysis results and shows quality of curve fitting process. It can be determined by using the equation given below;

$$R^2 = \frac{SS_R}{S_{yy}} = \frac{\sum_{j=1}^n (\hat{y}_j - \bar{y})^2}{\sum_{j=1}^n (y_j - \bar{y})^2} \quad (3.3)$$

In this equation;

$y_i - \bar{y}$ = Difference between i^{th} data point and mean value.

$\hat{y}_i - \bar{y}$ = Difference between i^{th} predicted value and mean value.

In our model the results of coefficient of determination (R^2) ranges from 0.5 to 0.63. Actually these two values show that the predicted parameters fit the data within the acceptable error ranges [11].

3.4. ESTIMATION of σ^2

Generally, it is necessary to obtain a good estimate of σ^2 in regression. The unbiased estimator, σ^2 , expresses variation in the residuals. The formula for σ^2 is given below [14].

$$\sigma^2 = \sum_{i=1}^n \frac{(y_i - \hat{y}_i)^2}{n - p} \quad (3.4)$$

In this formula, $y_i - \hat{y}_i$ is denotes the difference between i^{th} data point and predicted value, 'n' represents the number of data used in regression analysis y_i is the predicted or fitted response at the i^{th} data point and p is the number of parameters estimated. In our case, n is equal to 47 and p is equal to 7 (b1, b2, b3, b5, b_v, V_A, h).

Once the relationships were defined, the database was used to compute standard errors for PGA and PSA for each individual period. The standard deviation of the (ln) residuals (σ), expressing the random variability of ground motions, is an important input parameter in probabilistic hazard analysis. As mentioned before, in this study the observed value of $\ln\sigma$ lies within the range of 0.5 to 0.7.

The attenuation relationship obtained for PGA is graphically described as expected peak horizontal acceleration versus distance for three different soil conditions, several different magnitudes and compared with the attenuation formula of Boore et al. (1997) with applying actual earthquake data in Figure 3.11 through 3.19. In these figures +/-1 sigma curves are also presented.

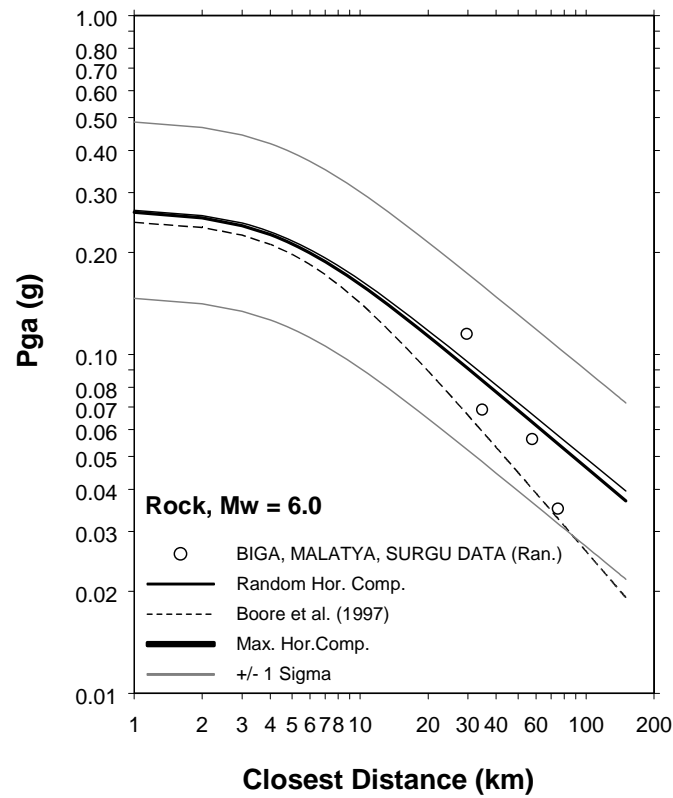
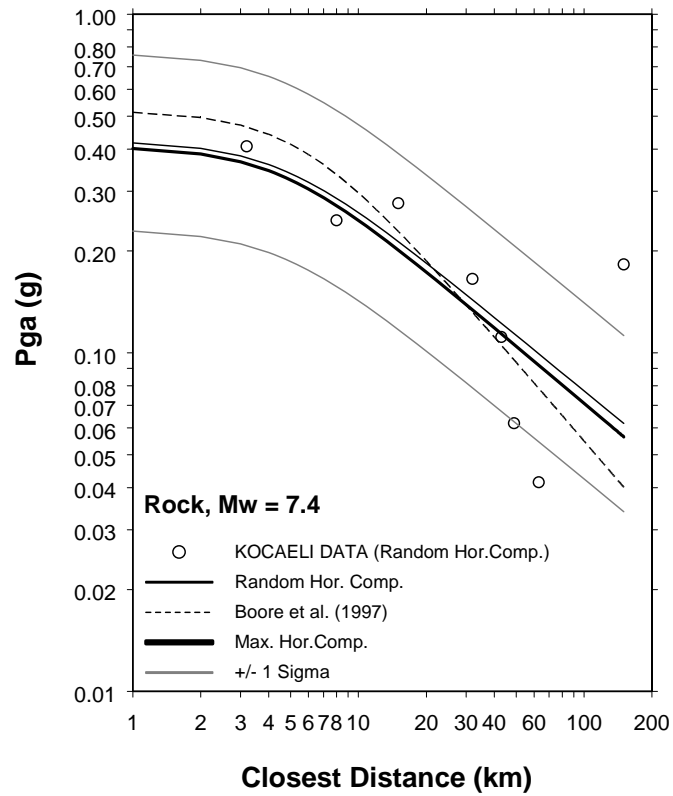


Figure 3.11 Curves of peak acceleration versus distance for magnitude 7.4 and 6.0 earthquakes at rock sites

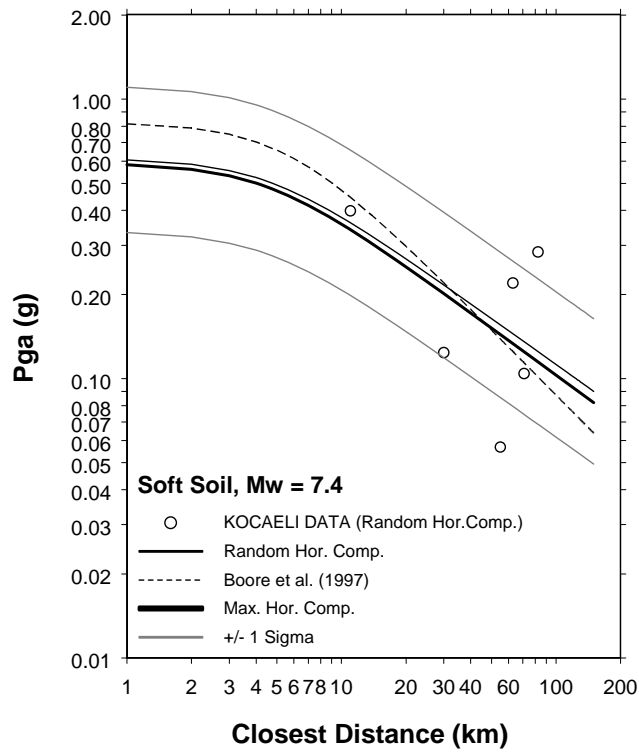
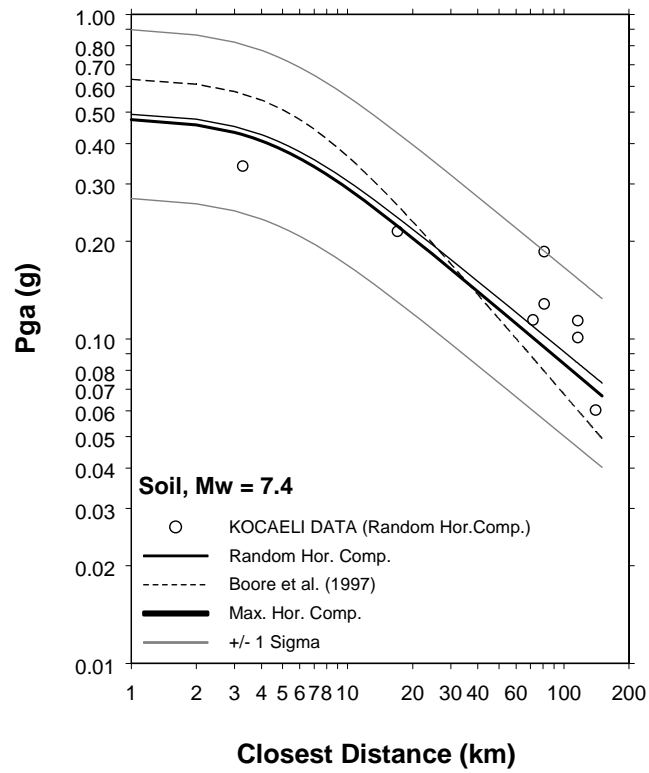


Figure 3.12 Curves of peak acceleration versus distance for magnitude 7.4 earthquakes at soil and soft soil sites

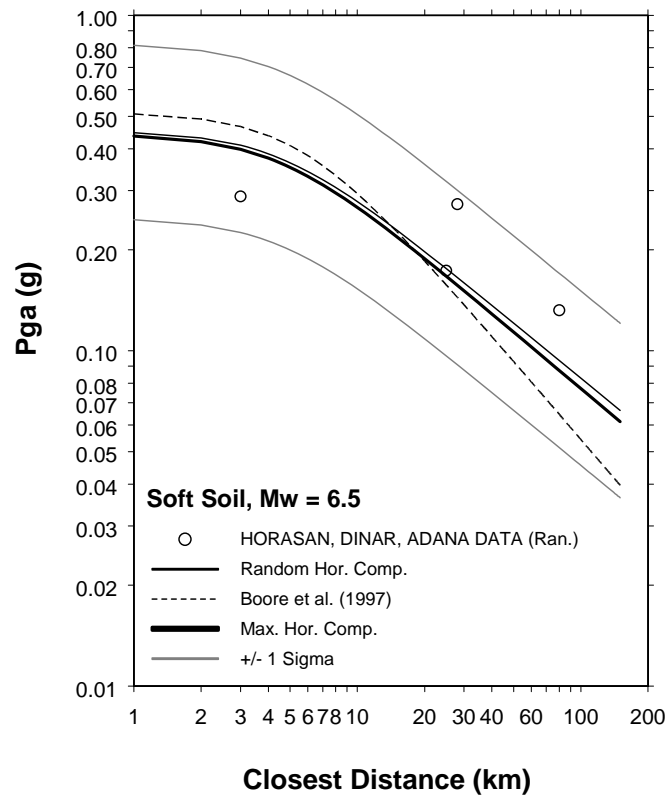


Figure 3.13 Curves of peak acceleration versus distance for magnitude 7.4 earthquake at soft soil site

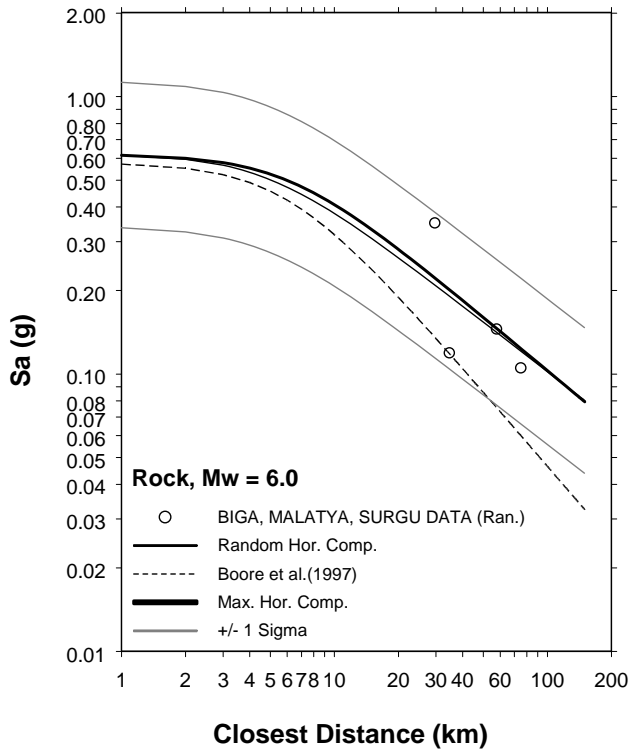
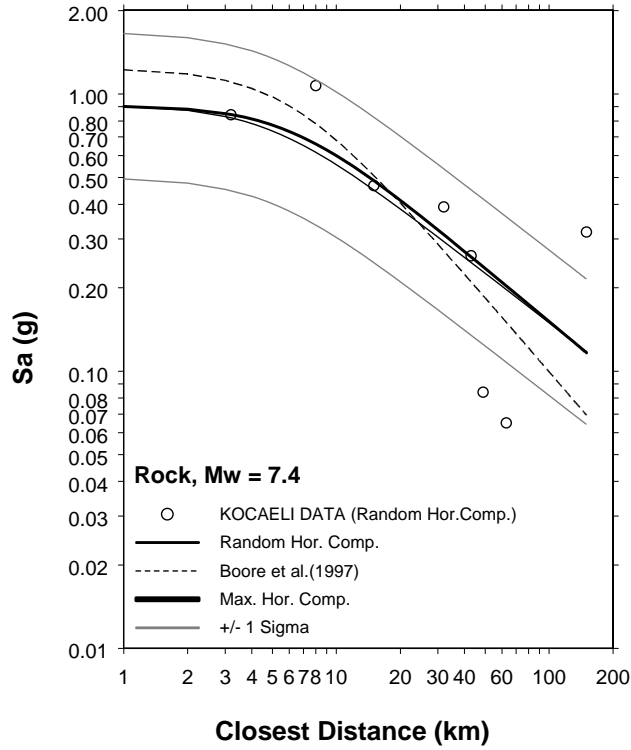


Figure 3.14 Curves of spectral acceleration at $T = 0.3s$ versus distance for magnitude 7.4 and 6.0 earthquakes at rock sites

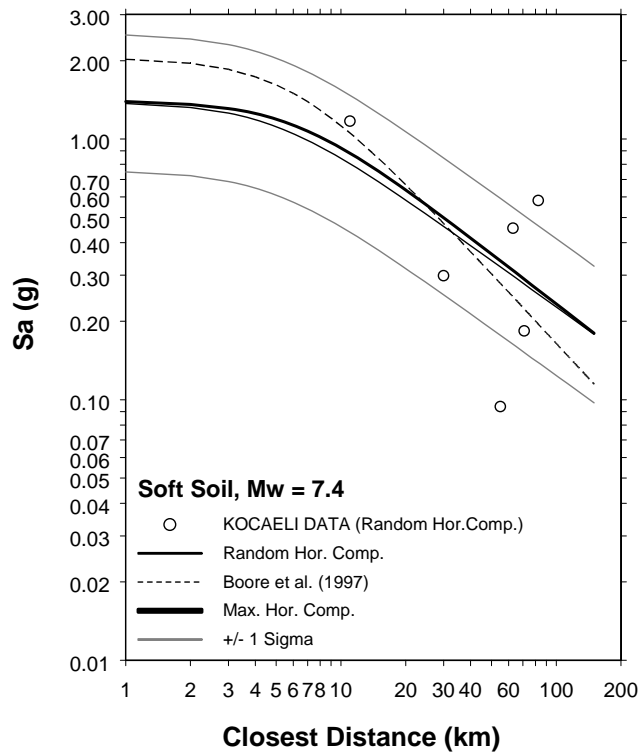
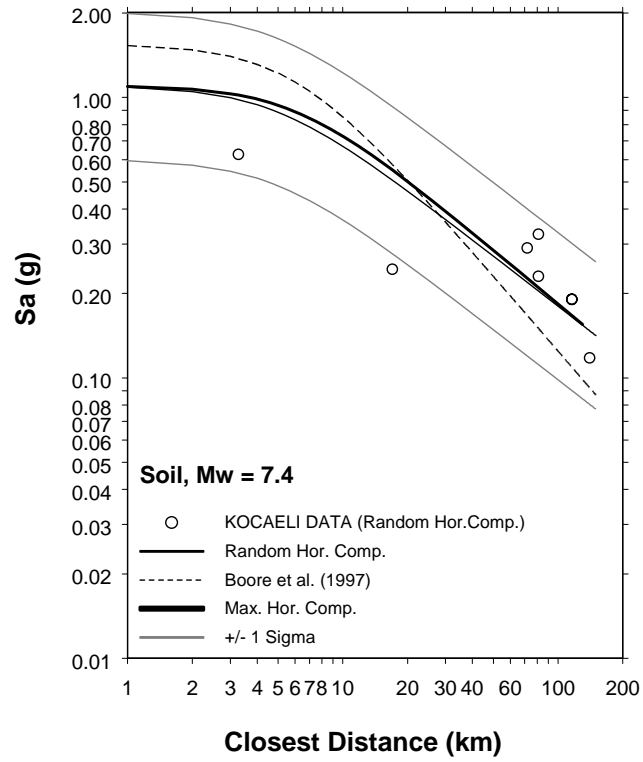


Figure 3.15 Curves of spectral acceleration at $T = 0.3s$ versus distance for magnitude 7.4 earthquake at soil and soft soil sites

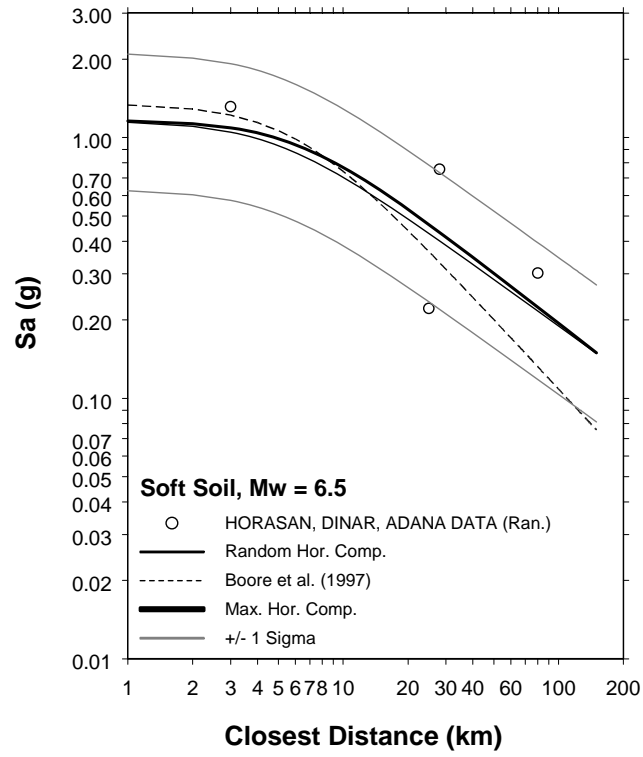


Figure 3.16 Curves of spectral acceleration at $T = 0.3s$ versus distance for magnitude 6.5 earthquake at soft soil site

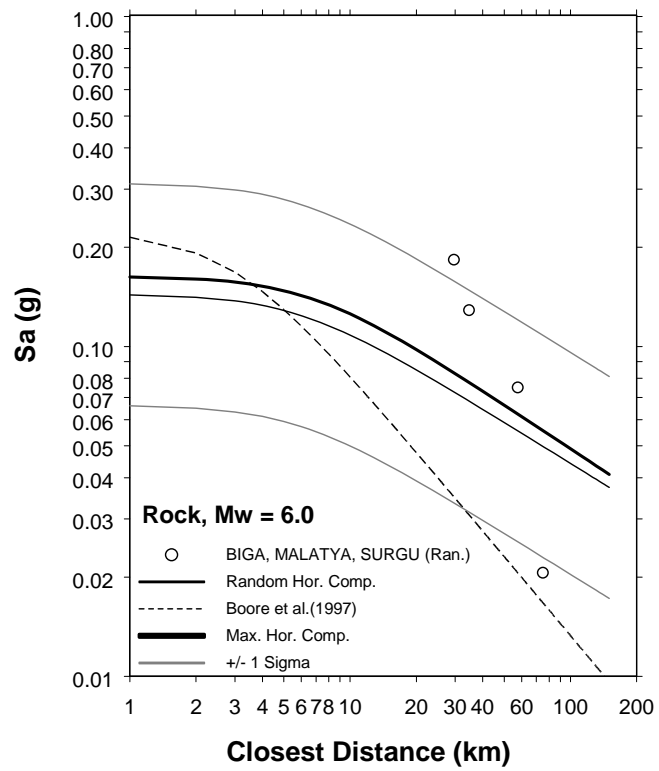
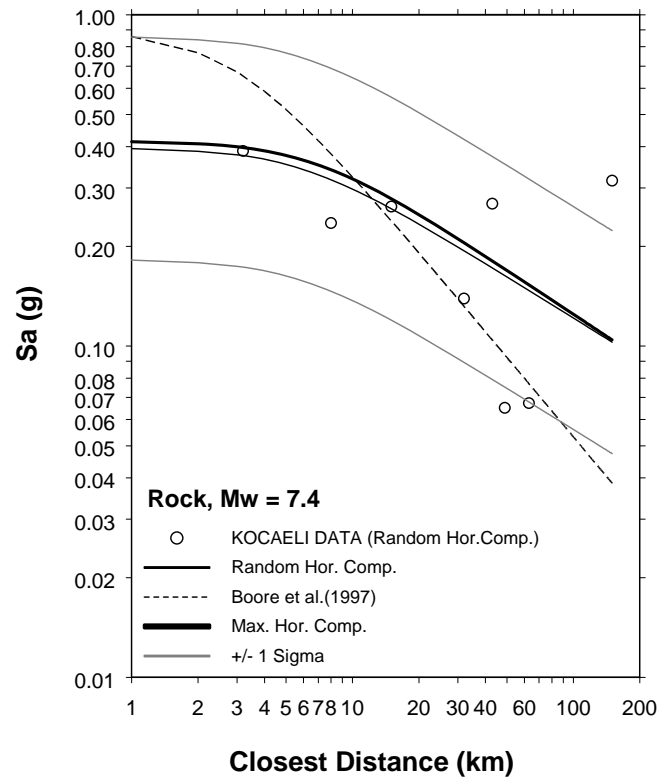


Figure 3.17 Curves of spectral acceleration at T = 1.0s versus distance for magnitude 7.4 and 6.0 earthquakes at rock sites

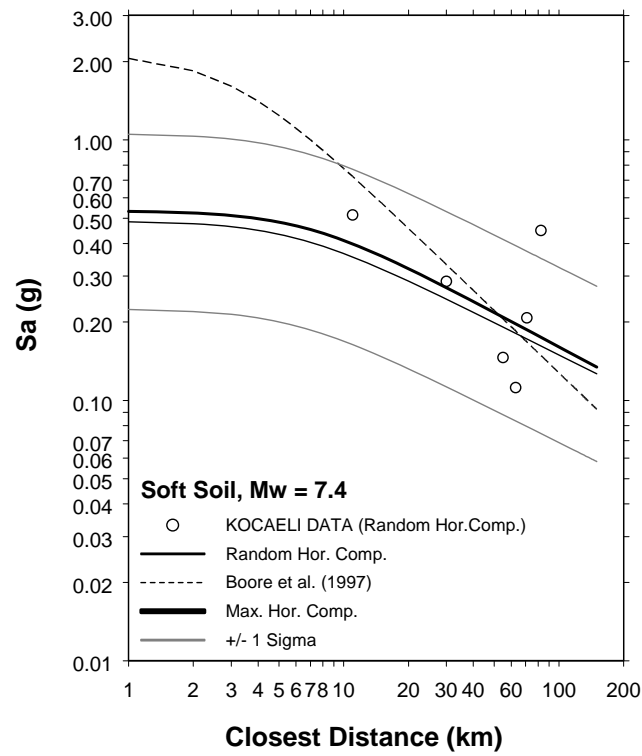
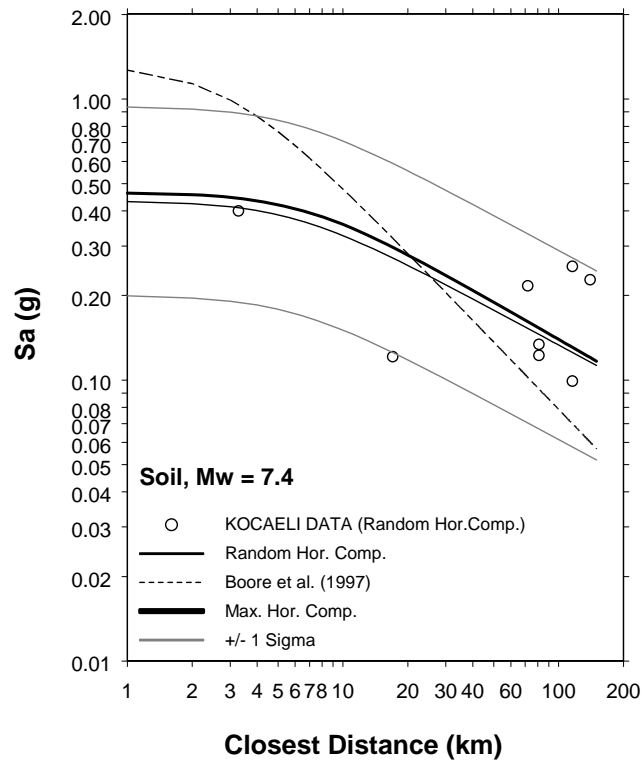


Figure 3.18 Curves of spectral acceleration at $T = 1.0s$ versus distance for magnitude 7.4 earthquake at soil and soft soil sites

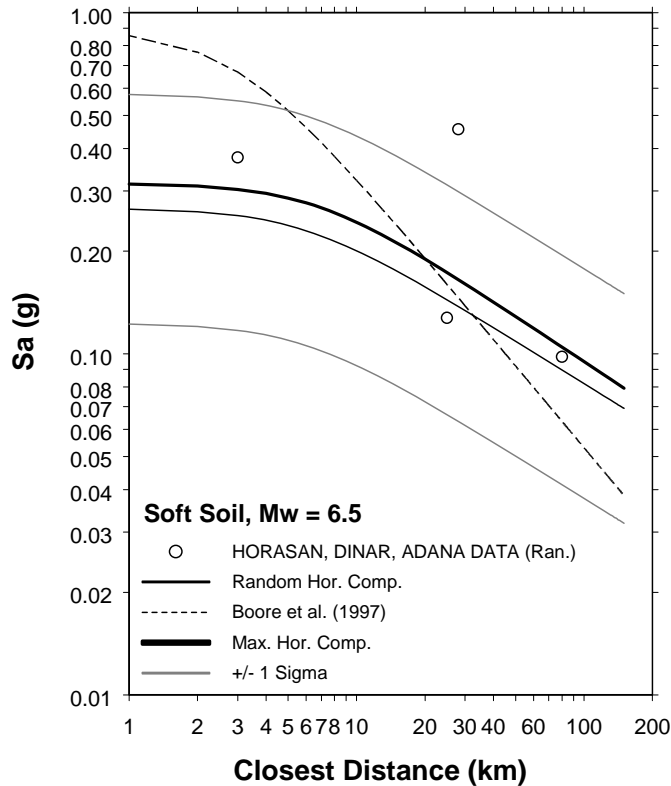


Figure 3.19 Curves of spectral acceleration at $T = 1.0s$ versus distance for magnitude 6.5 earthquake at soft soil site

3.5. COMPARISONS WITH OTHER GROUND MOTION RELATIONSHIPS

The estimate equations developed in this study are next compared to those recently developed by Boore et al. (1997), Campbell (1997), Sadigh et al. (1997), Spudich et al. (1997) and finally Ambraseys et al. (1996). The equations of Boore et al. (1997) and Ambraseys et al. (1996) divided site classes into four groups according to shear wave velocities. Campbell's equations pertain to alluvium (or firm soil), soft rock and hard rock. Sadigh et al. (1997) and Spudich et al. (1997) state that their equations are applicable for rock and soil sites.

The attenuation of PGA and PSA at 0.3 and 1.0 s for $M_w = 7.4$ for rock and soil sites are compared in Figures 3.20 to 3.22, respectively. The measured points from the Kocaeli event are also marked on these curves to illustrate how well they fit the

estimates. The differences in these curves are judged to be reasonable because different databases, regression models and analysis methods, different definitions for source to site distance and magnitude parameters among the relationships contained in each model.

For some parameters, and especially for PGA, there are numerous published attenuation equations for use in any particular engineering application. Atkinson and Boore (1997) showed the differences between attenuation characteristics in western and eastern USA for stable intraplate and interplate regions. Nevertheless, differences among attenuation of strong motions from one region to another have not been definitely proven. Because of this reason it is preferable to use attenuation equations that are based on the records taken from the region in which the estimation equations are planned to be applied.

Sensors comprising the national or other strong motion networks in Turkey are oriented so that their horizontal axes match the N-S and the E-W directions. Whereas Figure 2.7 illustrates the larger of these two components as a function of distance, it may not represent the largest horizontal acceleration that occurred before the cessation of the ground motion. The value of the absolute maximum acceleration in whichever direction can be determined by monitoring through a simple bookkeeping procedure for the size of the resultant horizontal component, and then resolving all pairs to the direction of that largest component once it is known. At variance with the customary practice, this component is called the “random” horizontal component. In Figure 3.23, the difference in the predictive power of the regression equations derived from both of these definitions is illustrated for $M_w = 7.4$, and compared against the Kocaeli measurements. It is believed that both sets yield essentially the same results. With the differences between the mean or the standard deviation curves substantially less than the value of $\ln(\sigma)$ itself, an improvement in accuracy does not appear to be plausible between the definitions of maximum horizontal acceleration.

When derived equations are compared with other attenuation relationships not developed specifically from recordings in Turkey, it is concluded that they overestimate the peak and spectral acceleration values for up to about 15-20 km. Trends of proposed curves are generally above these curves for larger distances because for expressions used in this study the fall-off trend is less strong. It is surmised that clipping the minimum peak acceleration at 0.04 g is the cause of this trend. Among the other attenuation relationships that have been used for comparison of the equations by Ambraseys et al. (1996) for European earthquakes yields better match with proposed equations. Whether this is caused by the fact that the Ambraseys study utilized data recorded also in Turkey cannot be answered except on a conjectural basis. But this comparison clearly serves as a reminder that there exists little support for the carefree import of attenuation curves from other environments for use in important engineering applications elsewhere.

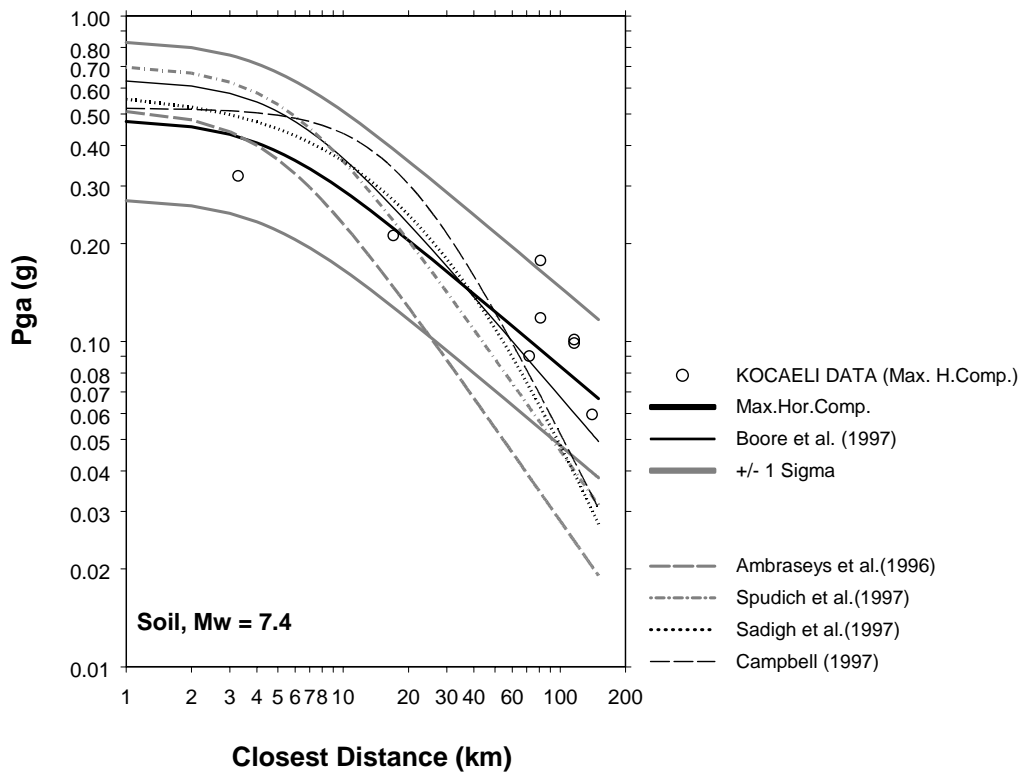
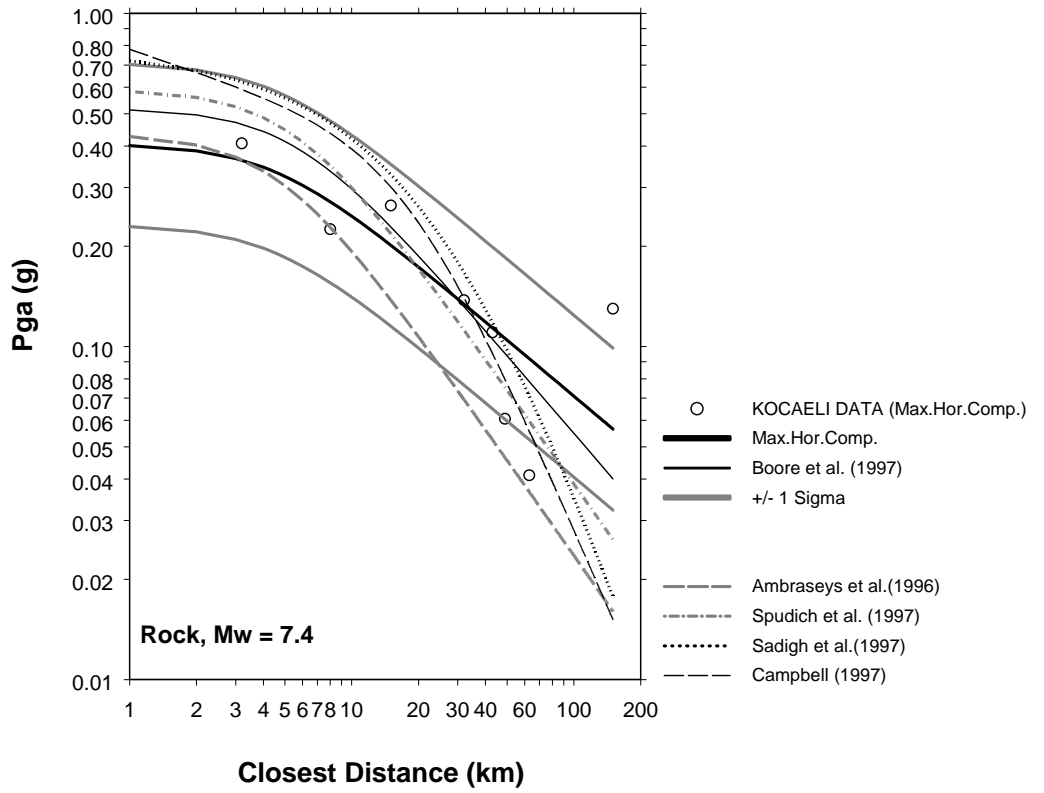


Figure 3.20 Curves of peak acceleration versus distance for magnitude 7.4 earthquakes at rock and soil sites

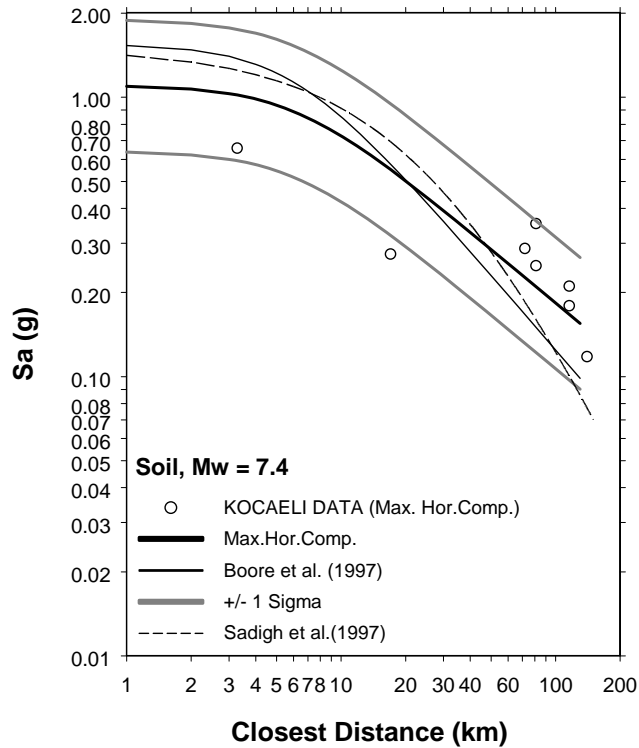
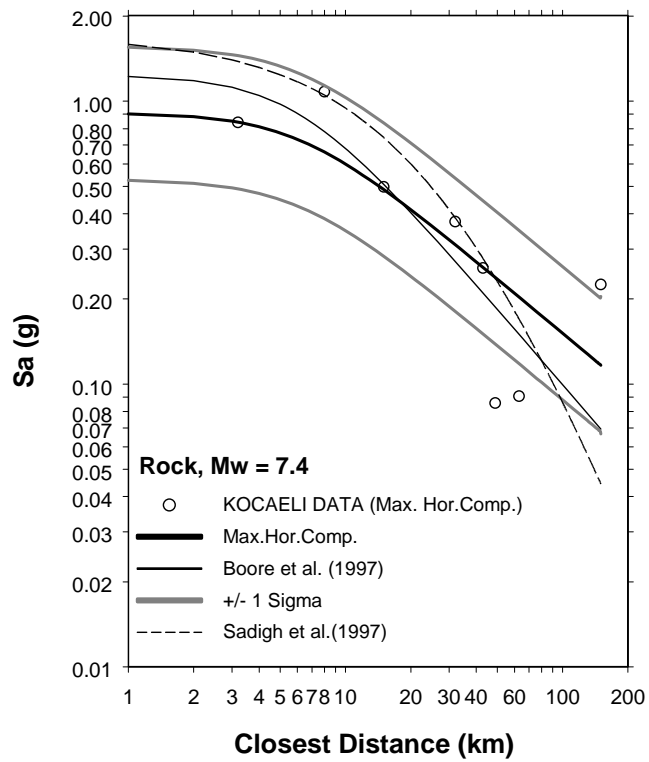


Figure 3.21 Curves of spectral acceleration at $T = 0.3$ s versus distance for a magnitude- 7.4 earthquake at rock and soil sites

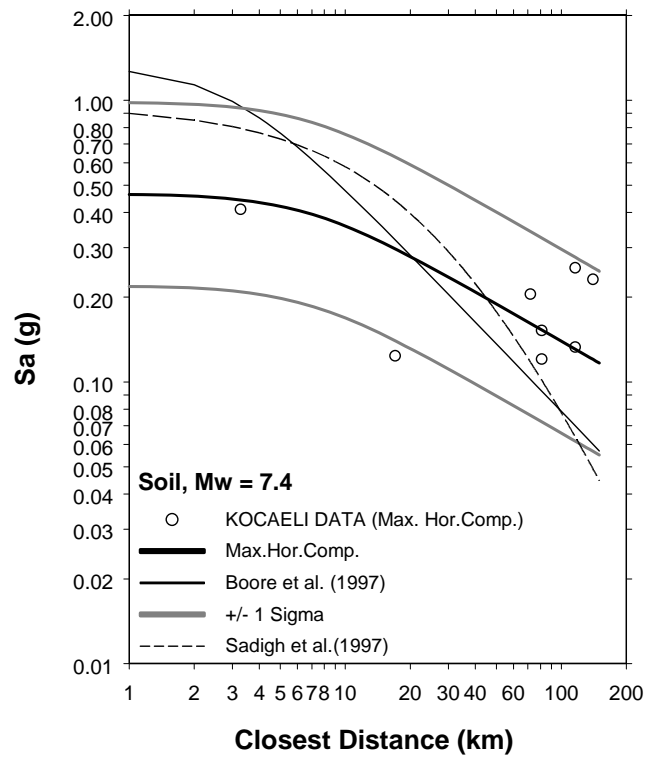
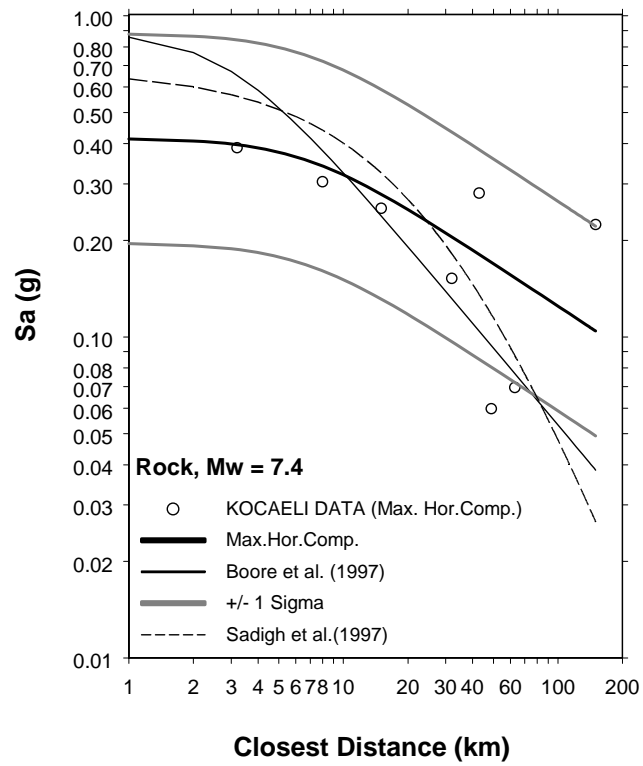


Figure 3.22 Curves of spectral acceleration at $T = 1.0$ s versus distance for a magnitude-7.4 earthquake at rock and soil sites

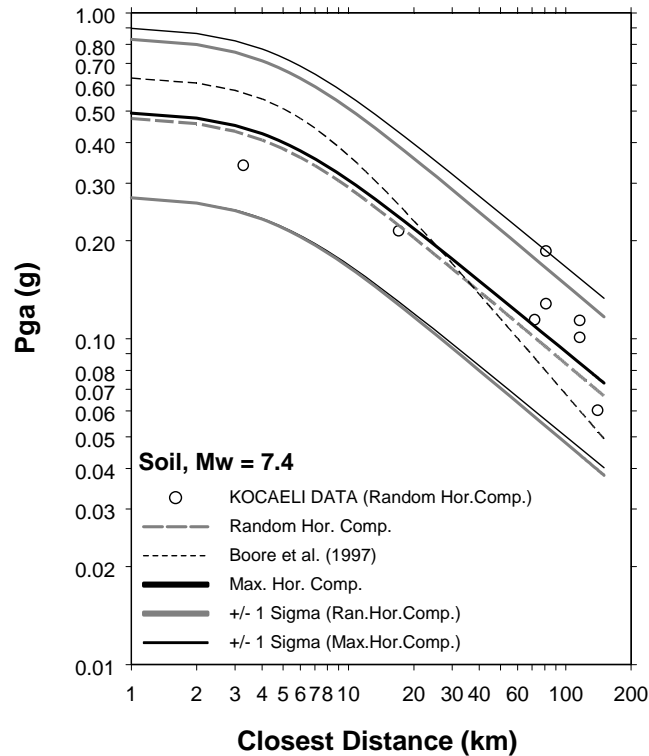


Figure 3.23 Differences caused by using the larger of the two horizontal components or the component in the direction of the largest resultant

3.6. UNCERTAINTY AND RELIABILITY

Uncertainty is a condition associated with essentially all aspects of earthquake related science and engineering. The principle sources of uncertainty lie in the characterization of site geology, in the calculation of closest distances, in the determination of seismic shaking properties and in the geotechnical properties of earthquake motion monitoring sites. The regression analysis is based on stochastic analysis method thus the obtained attenuation formula contains unavoidable errors.

It is customary in seismic hazard studies to distinguish between two types of uncertainty as follows [20]:

- *Epistemic Uncertainty:* This defines uncertainty that is due to incomplete knowledge and data about the physics of the earthquake process. In principle,

epistemic uncertainty can be reduced by the collection of additional information.

- *Aleatory Uncertainty*: Refers to uncertainty that is inherent to the unpredictable nature of future events. It represents unique details of source, path, and site response that cannot be quantified before the earthquake occurs. Aleatory uncertainty cannot be reduced by collection of additional information. One may be able, however, to obtain better estimates of the aleatory uncertainty by using additional data.

This study will refer to the combined epistemic and aleatory uncertainty as total uncertainty (or simply uncertainty). These uncertainties, for the most part stemming from the lack of and/or the imperfect reliability of the specific supporting data available, affect all analytical methods and procedures applied to the derivation of all aforementioned estimating parameters.

The attenuation relationships presented in this study cannot, and do not, eliminate these uncertainties. However through the use of nonlinear regression analysis, it provides a more sophisticated and direct approach to address the uncertainties than do traditional linear analysis procedures. The results presented in tabular and graphical form become meaningful only in the context of the error distributions that are associated with each variable. In general, results of this study possess larger deviations in comparison with, e.g., Boore et al. (1997). This is plausible because of the smaller number of records from which they have been derived. In view of the limited number of records utilized in this study it may not be appropriate to expect the distributions to conform to the normal distribution. It is utilized only as a tool that permits a direct comparison to be made between obtained results and those of Boore et al. (1997).

CHAPTER 4

EARTHQUAKE HAZARD AND SITE-DEPENDENT RESPONSE SPECTRA

4.1. GENERAL

The hazards imposed by earthquakes are unique in many respects, and consequently, planning to mitigate earthquake hazards requires a unique engineering approach. The majority of damage caused by earthquakes, especially to buildings, can be directly attributed the effects of ground shaking induced by the passage of seismic waves. Estimation of the maximum effects and consequently maximum damage, especially related with ground motion parameters of postulated earthquakes within specific boundaries is therefore fundamental and essential for mitigating the earthquake hazard in the future. For this aim seismic risk procedures and attenuation relationships are mostly developed for defining the damage at the site by estimating peak horizontal accelerations.

In order to minimize the consequences of anticipated earthquakes and make safer designs, a tool known as design spectrum is widely used. In this study, for the development of design spectra for Turkey, the data obtained from attenuation relationships for different site conditions were utilized.

4.2. SITE-DEPENDENT RESPONSE SPECTRA

The maximum values of the ground motion (peak ground acceleration, peak ground velocity, and peak ground displacement) are of interest in seismic analysis and design. These parameters, however, do not by themselves describe the intensity of shaking. Other factors, such as the earthquake magnitude, distance from fault or

epicenter, duration of strong shaking, soil condition of the site, and frequency content of the motion also influence the response of a structure. Some of these effects, such as amplitude of motion, duration of strong shaking, frequency content, and local soil conditions are best represented through the response spectrum, which describes the maximum response of a damped single-degree-of-freedom oscillator to various frequencies or periods. In this study only the elastic spectrum is considered.

Engineers and seismologists have long recognized the importance of response spectra as a means of characterizing the ground motions produced by earthquakes and their effects on structures. Since the concept of a response spectrum was first introduced by Housner (1941) and Biot (1942), spectra have been widely used for the purposes of differentiating between the significant characteristics of accelerograph records and providing a simple method of evaluating the response of all types of structures to ground shaking. Newmark and Hall (1973) recommended straight lines be used to represent earthquake design spectra. They suggested that three amplification factors which are constant in the high, intermediate, and low frequency regions of the spectrum, together with peak ground acceleration, velocity and displacement be used to construct normalized design spectra [24].

While response spectra for a specified earthquake record may be used to obtain the response of a structure to an earthquake ground motion with similar characteristics, they can not be used for design, because response of the same structure to another earthquake will undoubtedly be different. Nevertheless, the recorded ground motion and computed response spectra of past earthquakes exhibit certain similarities. For example, studies have shown that response spectra from accelerograms recorded on similar soil conditions reflect similarities in shape and amplifications [2]. For this reason, attenuation relationships to obtain response spectra for specific regions for design become very useful tools.

To provide an indication of the differences in site-dependent spectra, response spectra for rock, soil and soft soil site classes were computed for several values of M_w and r_{cl} by substituting these values into the equations derived in the previous section (see Table 3.1). Typical examples are shown in Figure 4.1 through

Figure 4.9 for M_w 6.5, 7.0 and 7.5 events at the closest distances of 5 km, 10 km and 15km, respectively.

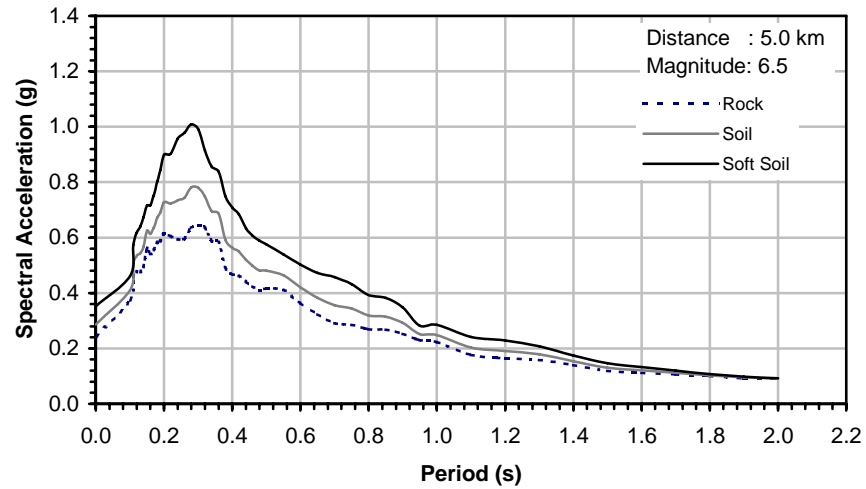


Figure 4.1 Mean response spectra for magnitude 6.5 earthquake at a distance of 5.0 km for various geological conditions

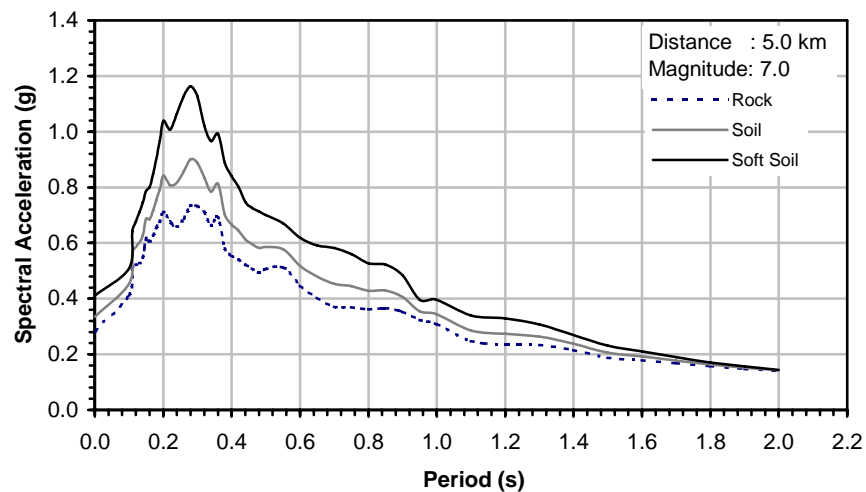


Figure 4.2 Mean response spectra for magnitude 7.0 earthquake at a distance of 5.0 km for various geological conditions

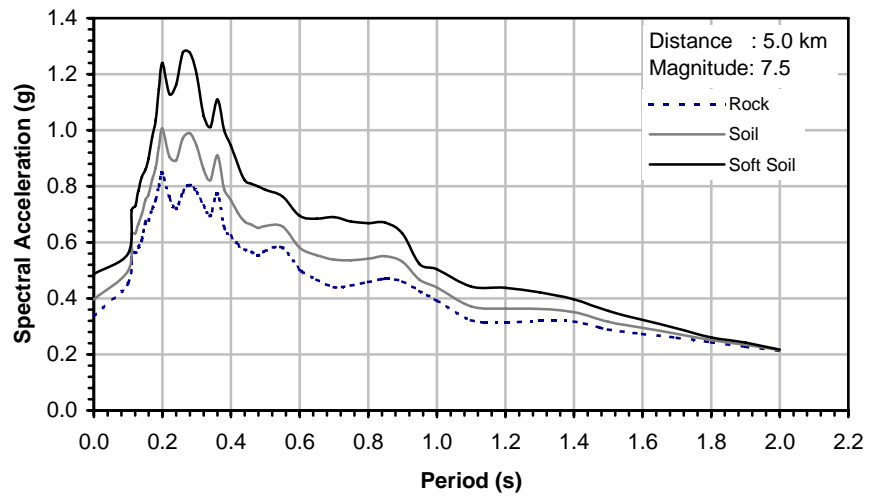


Figure 4.3 Mean response spectra for magnitude 7.5 earthquake at a distance of 5.0 km for various geological conditions

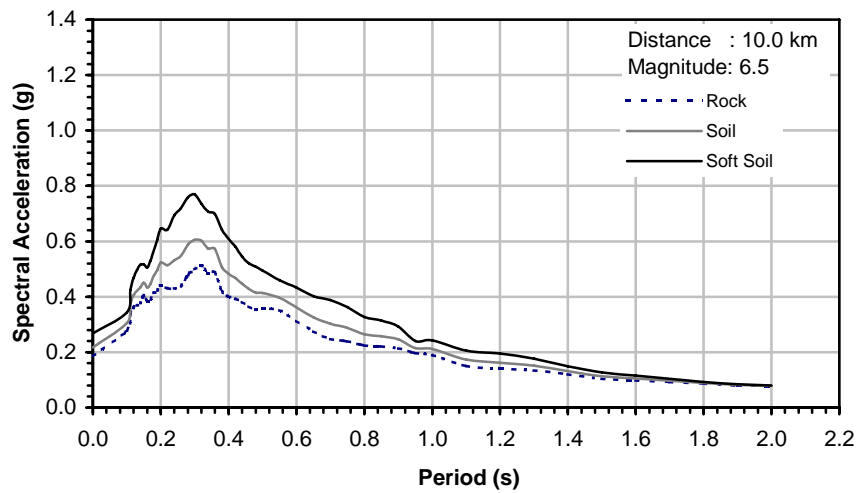


Figure 4.4 Mean response spectra for magnitude 6.5 earthquake at a distance of 10.0 km for various geological conditions

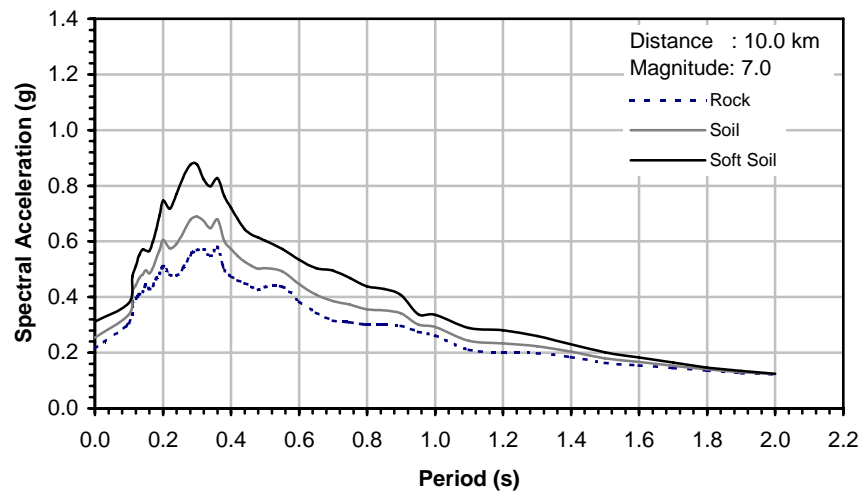


Figure 4.5 Mean response spectra for magnitude 7.0 earthquake at a distance of 10.0 km for various geological conditions

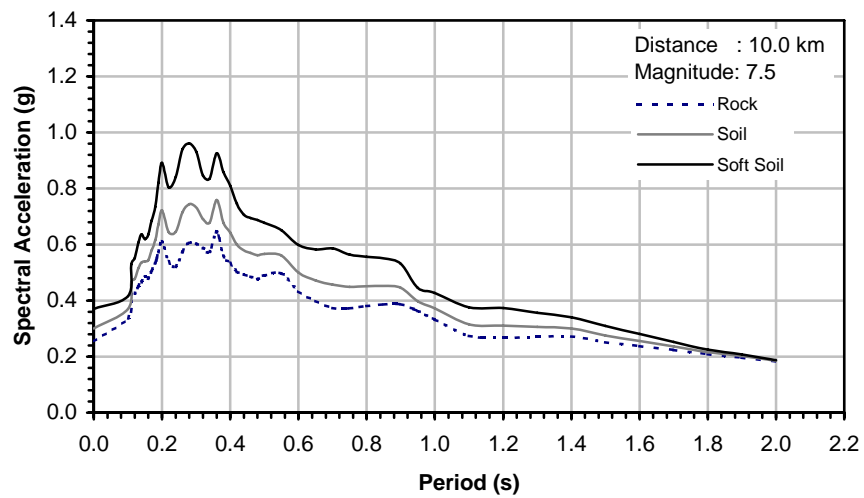


Figure 4.6 Mean response spectra for magnitude 7.5 earthquake at a distance of 10.0 km for various geological conditions

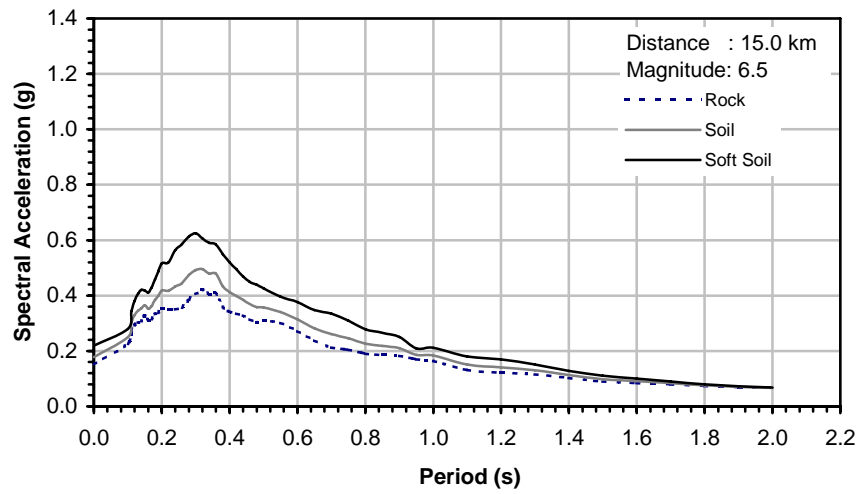


Figure 4.7 Mean response spectra for magnitude 6.5 earthquake at a distance of 15.0 km for various geological conditions

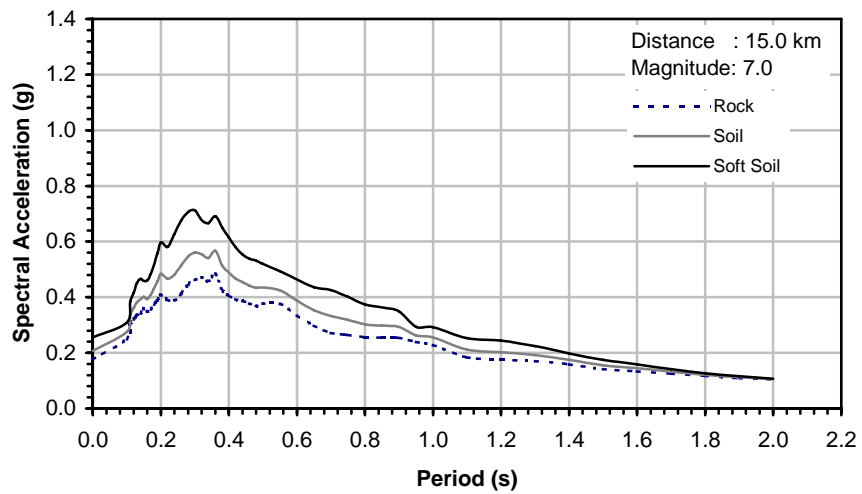


Figure 4.8 Mean response spectra for magnitude 7.0 earthquake at a distance of 15.0 km for various geological conditions

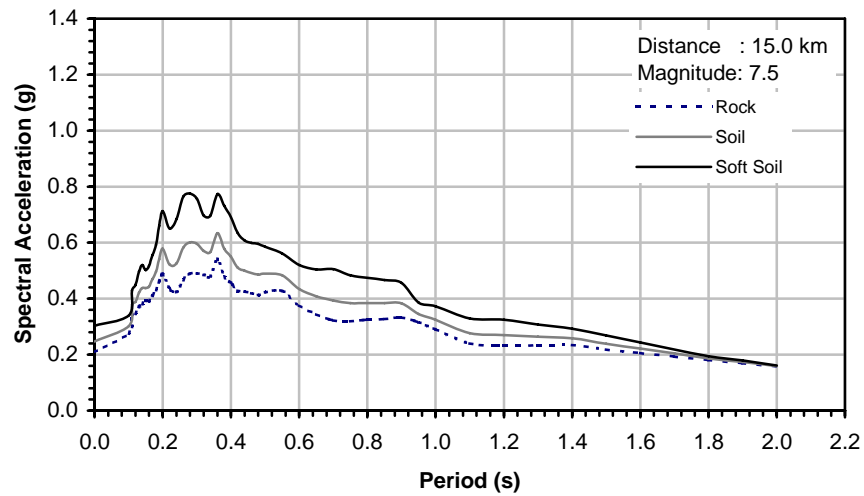


Figure 4.9 Mean response spectra for magnitude 7.5 earthquake at a distance of 15.0 km for various geological conditions

4.3. SMOOTH SITE-DEPENDENT RESPONSE SPECTRA

For practical applications, design spectra are presented as smooth curves or straight lines. Smoothing is justified because of the difficulties in determining the exact frequencies and mode shapes of structures during severe earthquakes when the behavior is most likely nonlinear. In this study, horizontal response spectra were smoothed according to detailed procedure described in FEMA273 [25]. In this method, a general, horizontal response spectrum may be constructed by plotting the following two functions in the spectral acceleration vs. structural period domain, as shown in Figure 4.10.

$$S_a = (S_{XS} / B_S)(0.4 + 3T / T_0) \quad \text{for } 0 < T < 0.2T_0 \quad (4.1)$$

$$S_a = (S_{X1} / B_1 T) \quad \text{for } T > T_0 \quad (4.2)$$

$$T_0 = (S_{X1} B_S) / (S_{XS} / B_1) \quad (4.3)$$

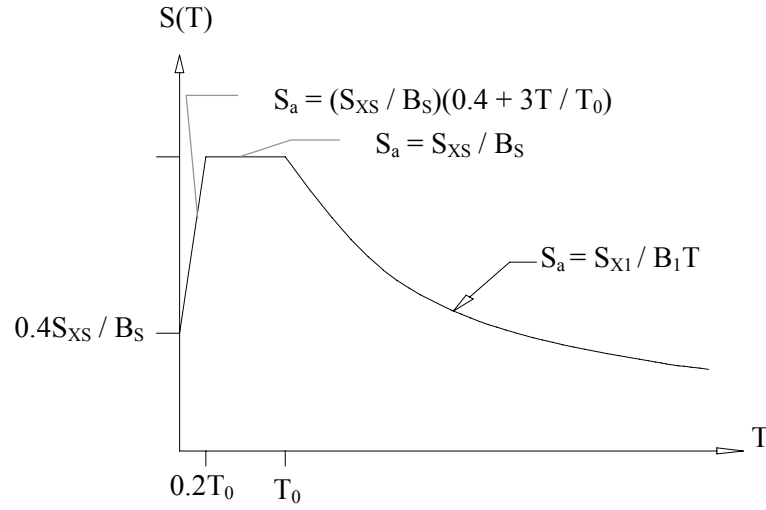


Figure 4.10 General response spectrum [25]

In these equations, B_S and B_1 are equal to 1 for 5% damping response spectrum. The value of the design spectral response acceleration at short periods, S_{XS} , shall be taken as the response acceleration obtained from the site-specific spectrum at period of 0.2 seconds, except that it should be taken as not less than 90% of the peak response acceleration at any period. In order to obtain a value for the design spectral response acceleration parameter S_{X1} , a curve of the form $S_a = S_{X1} / T$ should be graphically overlaid on the site-specific spectrum such that at any period, the value of S_a obtained from the curve is not less than 90% of that which would be obtained directly from the spectrum [25]. The value of T_0 shall be determined in accordance with Equation 4.4.

$$T_0 = S_{X1} / S_{XS} \quad (4.4)$$

Smoothed spectra according to procedure described are presented in Figures 4.11 through 4.13. With these spectra, one may establish a set of coefficients by which the ordinates of design spectra for rock sites could be multiplied to give design spectra for other site categories. The comparisons of the developed site-dependent response spectra from the obtained attenuation formulas with regulatory Turkish spectra and UBC 1997 are also presented.

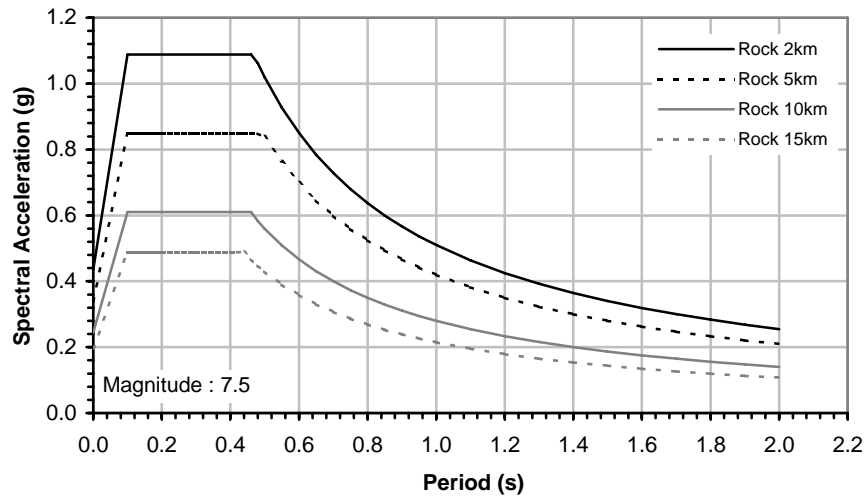


Figure 4.11 Smoothed mean spectra (5% damping) for magnitude 7.5 earthquake for various distances at rock sites

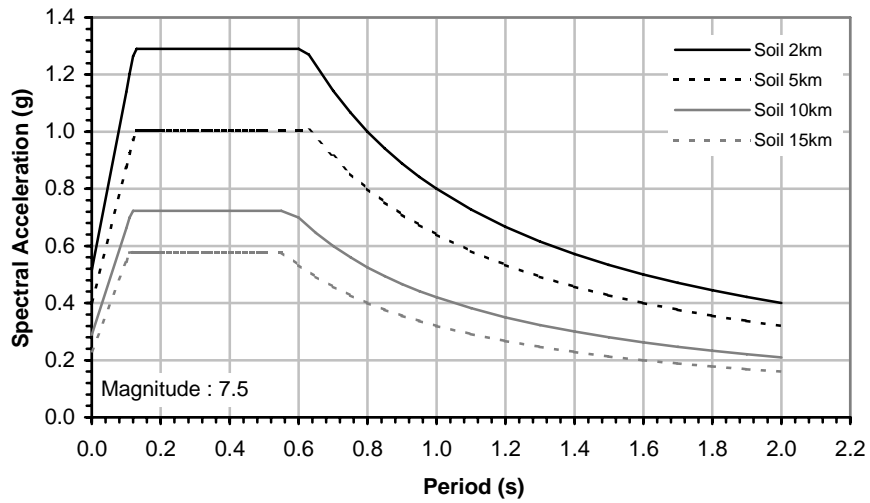


Figure 4.12 Smoothed mean spectra (5% damping) for magnitude 7.5 earthquake for various distances at soil sites

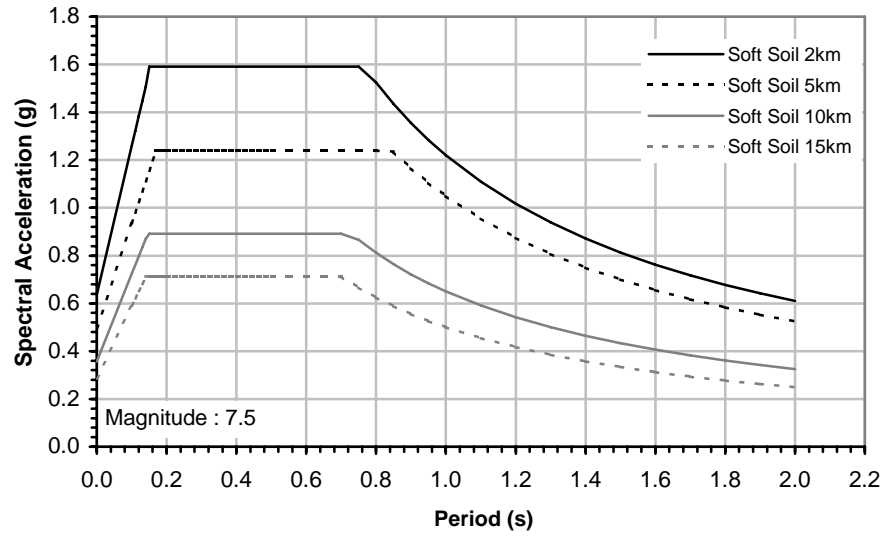


Figure 4.13 Smoothed mean spectra (5% damping) for magnitude 7.5 earthquake for various distances at soft soil sites

4.4. COMPARISONS WITH THE REGULATORY TURKISH SPECTRA

The Turkish seismic design code concerning the constructions in seismic areas has been recently modified in 1998. The recorded spectra for strong motions records of Dinar (1995) and several stations from the Kocaeli (1999) earthquakes are compared with this regulatory spectrum. The spectral acceleration coefficient, $A(T)$, corresponding to 5 percent damped elastic design acceleration spectrum normalized by the acceleration of gravity, g , is given by Equation (4.5) which shall be considered as the basis for the determination of seismic loads.

$$A(T) = A_0 \times I \times S(T) \quad (4.5)$$

Here, T is fundamental period of the building, $A_0 = 0.40$ (effective ground acceleration coefficient, for the seismic zone 1 in Turkey), $I = 1.0$ (building importance factor, value for the standard buildings), $S(T)$ is the spectrum coefficient, is determined by the following Equation (4.6), depending on the local site conditions and the building fundamental period, T , in this equation T_A and T_B correspond to the corner periods of smooth elastic acceleration spectrum, illustrated in Figure 4.14.

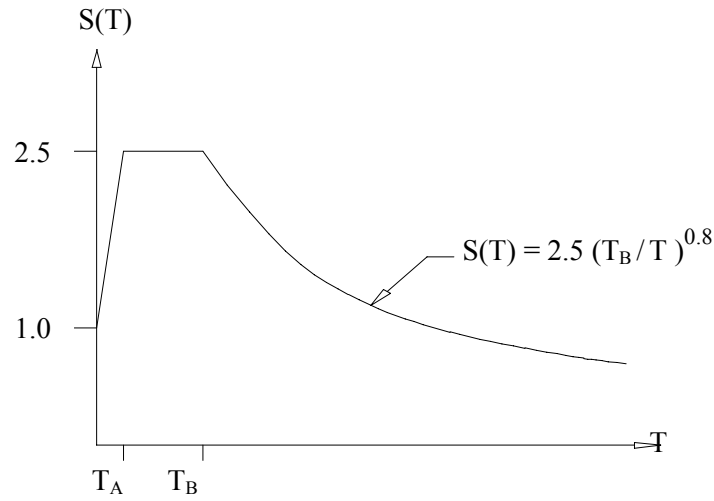


Figure 4.14 Code basis design acceleration spectrum for 5% damping [26]

$$S(T) = 1 + 1.5 T / T_A \quad (0 \leq T \leq T_A) \quad (4.6a)$$

$$S(T) = 2.5 \quad (T_A < T \leq T_B) \quad (4.6b)$$

$$S(T) = 2.5 (T_B / T)^{0.8} \quad (T > T_B) \quad (4.6c)$$

Elastic seismic loads to be determined in terms of spectral acceleration coefficient defined in (4.5) shall be divided by a seismic load reduction factor (R) defined below to account for the specific nonlinear behavior of the structural system during earthquake. In Turkey, R is equal to 4 for conventional buildings. Seismic load response modification factor, $R_a(T)$ shall be determined by Equations (4.7) in terms of structural behavior factor, R , and the fundamental period T .

$$R_a(T) = 1.5 + (R - 1.5) T / T_A \quad (0 \leq T \leq T_A) \quad (4.7a)$$

$$R_a(T) = R \quad (T > T_A) \quad (4.7b)$$

Therefore, elastic seismic loads are determined in terms of spectral acceleration coefficient by:

$$A_c(T) = A(T) / R_a(T) \quad (4.8)$$

The reason underlying the use of response modification factor is to design more economic buildings by considering their elasto-plastic limits and non-collapse mechanisms for desired seismic performance levels. When the spectra with this response modification factor are exceeded during an earthquake, it does not mean that the building with this spectrum will collapse, it implies rather than that it will no longer behave elastically, it may enter into the elasto-plastic domain of response.

For the comparison of derived site-dependent response spectra with regulatory Turkish Spectra, standard buildings are selected (with fundamental periods between 0.4s and 1.0s). These comparisons are shown in Figures from 4.15 through 4.19. For these comparisons near field records are intentionally selected. Note that the calculation of the spectra for rock conditions does not have an influence on the acceleration for zero period, it changes only the length of the plateau (longer for soil and soft soil conditions). The results derived from those figures show that the spectra computed from the recorded accelerations are usually close to “elastic” regulatory spectra for long periods and below the elastic regulatory spectra for low periods. The spectra including the response modification factor are considered as indicative of the minimum forces to be taken into account by the design engineers. However, all the spectra with this factor are always lower than the recorded accelerations, especially for 0.1s and 1.5s. This period range is typical for the fundamental periods of majority of the buildings in high-active zones of Turkey (number of floors less than 15).

All these results show that for standard residential buildings, the regulatory spectra (including the response modification factor) are below the spectra computed from the recorded accelerations whereas the derived site-dependent response spectra in this study well agree with recorded acceleration response spectra.

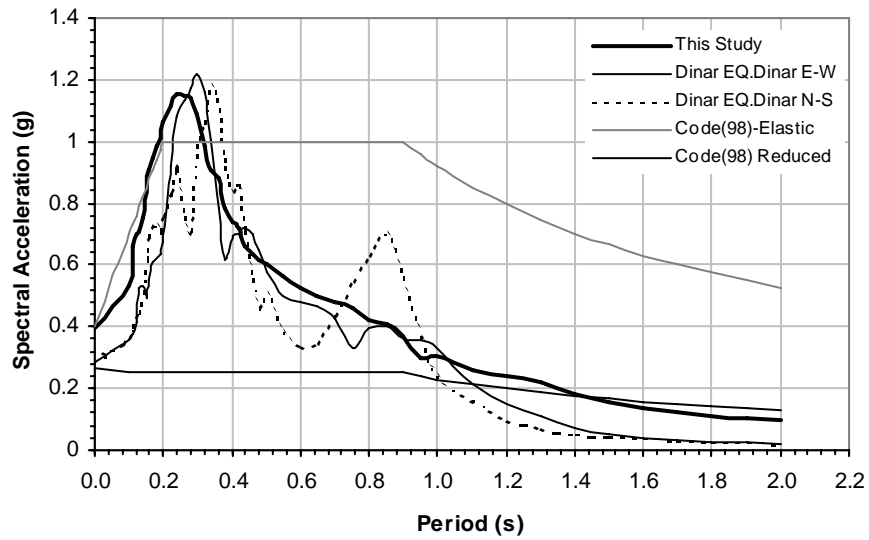


Figure 4.15 Comparison of proposed design spectra for 5 percent of critical damping and computed response spectra for the N-S and E-W components of Dinar, Dinar Earthquake of 1995, ($M_w = 6.5$, Soft soil)

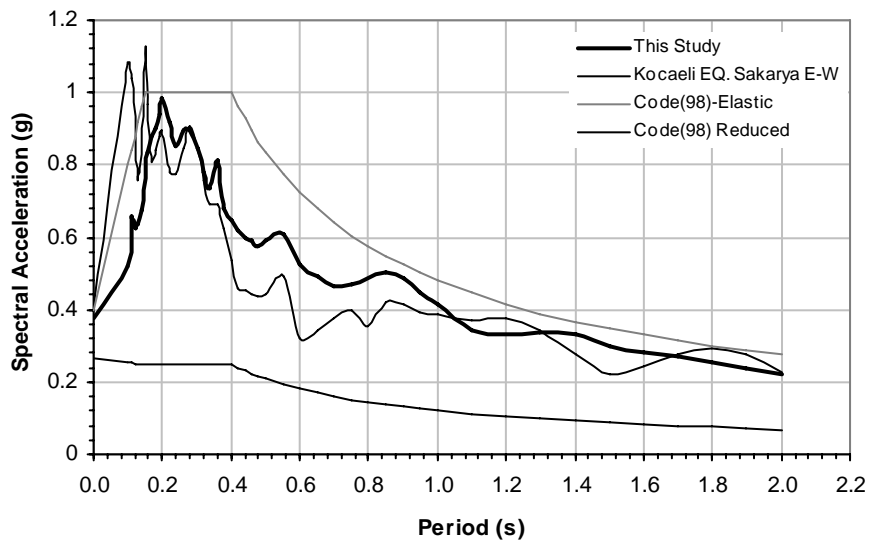


Figure 4.16 Comparison of proposed design spectra for 5 percent of critical damping and computed response spectra for the E-W component of Sakarya, Kocaeli Earthquake of 1999, ($M_w = 7.4$, Rock)

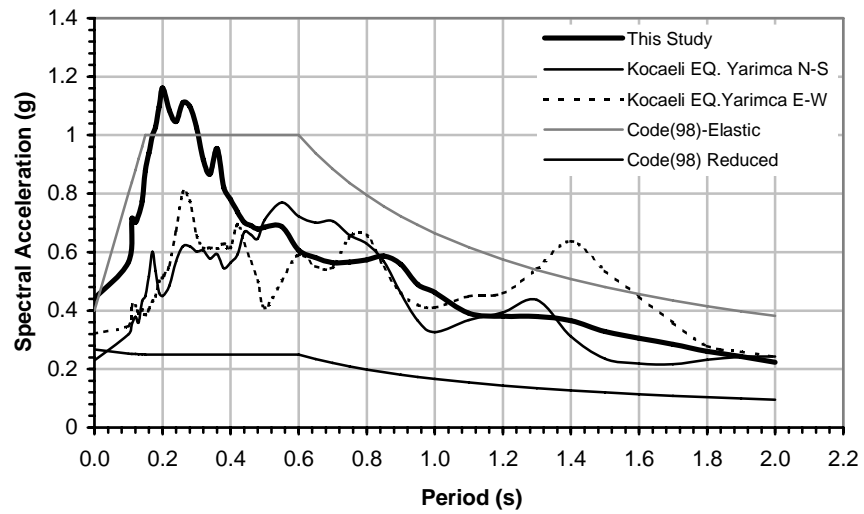


Figure 4.17 Comparison of proposed design spectra for 5 percent of critical damping and computed response spectra for the N-S and E-W components of Yarimca, Kocaeli Earthquake of 1999, ($M_w = 7.4$, Soil)

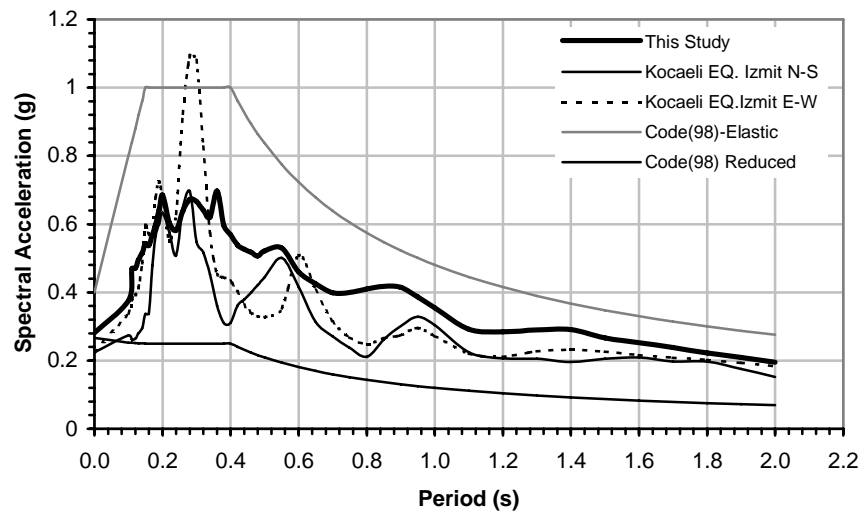


Figure 4.18 Comparison of proposed design spectra for 5 percent of critical damping and computed response spectra for the N-S and E-W components of İzmit, Kocaeli Earthquake of 1999, ($M_w = 7.4$, Rock)

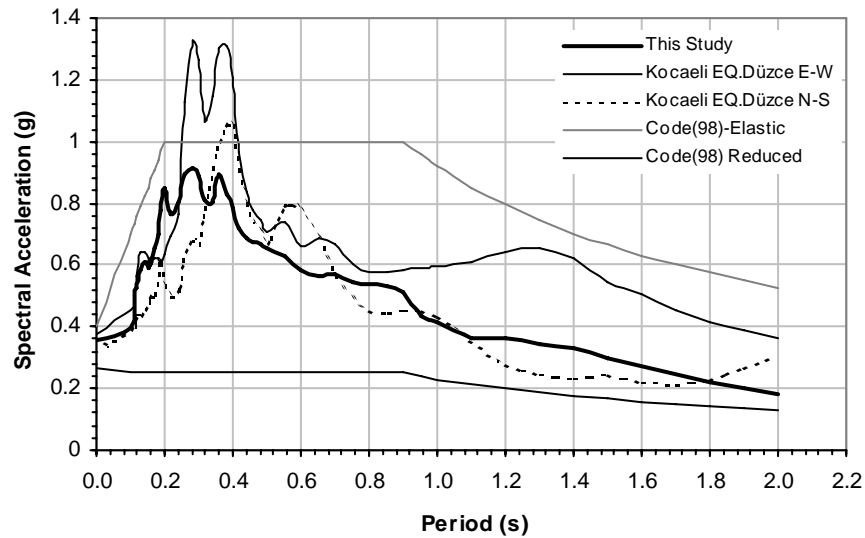


Figure 4.19 Comparison of proposed design spectra for 5 percent of critical damping and computed response spectra for the N-S and E-W components of Düzce, Kocaeli Earthquake of 1999, ($M_w = 7.4$, Soft soil)

The mean response spectra given in Figures 4.11 to 4.13 were normalized to a unit (1.0g) horizontal ground acceleration by dividing spectral acceleration values with their PGA values. When the current code design spectra are compared with those proposed normalized smooth spectra for magnitude 7.5, which can be accepted as a design earthquake level for highly seismic regions in Turkey, it is concluded that code spectra overestimate the spectral acceleration values past about 10 km. Trends of proposed curves are slightly above these curves for smaller distances and below these curves after 10 km. These comparisons are presented in Figure 4.20 and 4.21 for various geological conditions and distance values. In these figures Z1, Z2, Z3 and Z4 denote the code site classification in ascending order from hard rock to soft soil. With the proviso that the code categories for soils do not necessarily match the assigned shear wave velocities used in the derivation of the attenuation curves, the agreement is within acceptable limits. As a result of all these comparisons it can be concluded that use of given attenuation relationships for Turkey in this study presents more reliable and consistent seismic loads for possible use in the design of engineered buildings.

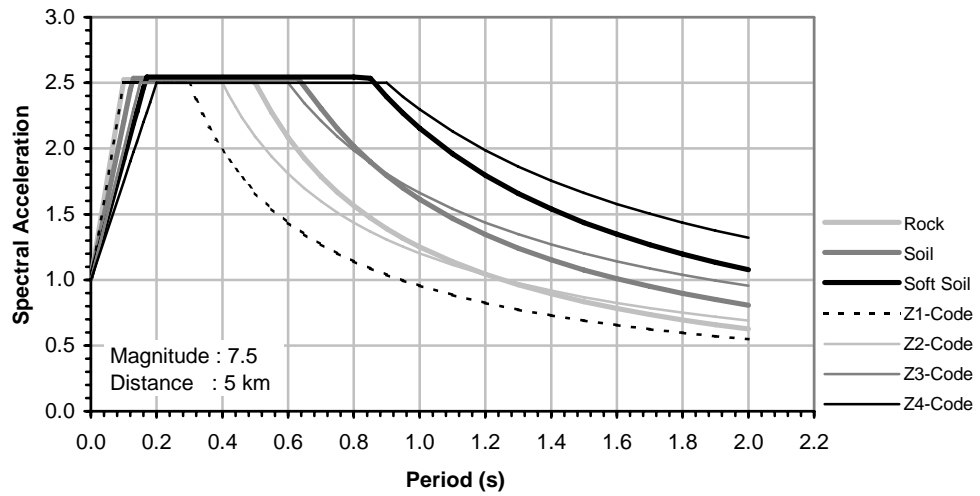


Figure 4.20 Comparison of proposed smooth spectra for 5 percent of critical damping and current seismic code for various geological conditions

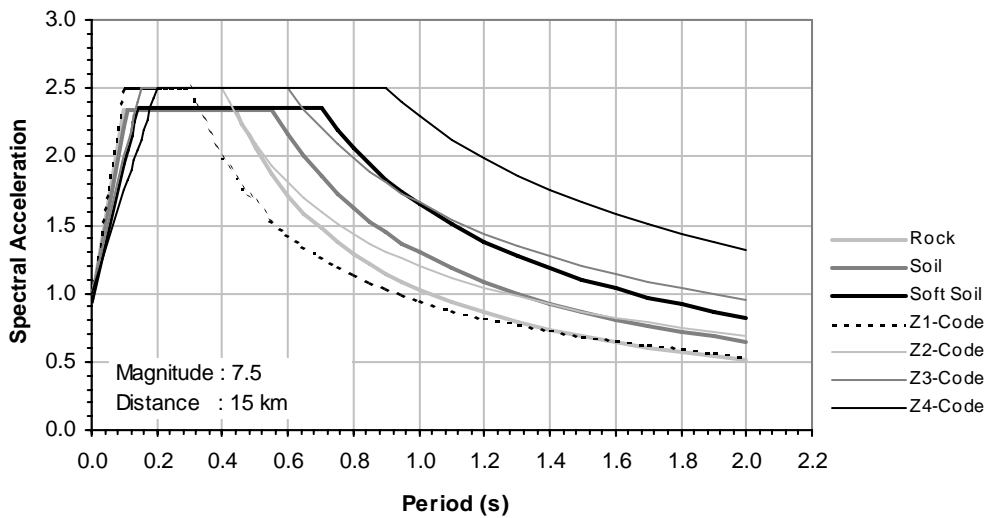


Figure 4.21 Comparison of proposed smooth spectra for 5 percent of critical damping and current seismic code for various geological conditions

Another inconsistency for the Turkish code is the arbitrary and baseless use of the 0.8 power for the falling branch of the design spectrum. This factor contradicts the spectrum concept, and is clearly on the conservative side by a large

margin. Conversely, the corner periods for rock or very stiff soil sites correspond to a very narrow plateau, and are not supported by the data at hand. This deficiency should also be addressed when code revisions are considered.

4.5. COMPARISONS WITH UBC 1997 RESPONSE SPECTRA

The smooth design spectra developed in this study were compared to those developed by UBC 1997. The normalized spectra are compared for various geological conditions for distance of 2 km and 10 km in Figure 4.22 and 4.23. In Figure 4.24, the comparisons of smooth spectra are also presented. These figures compare the mean spectral shapes obtained for rock, soil and soft soil site conditions with those obtained for similar geological conditions classified according to their shear wave velocities by UBC 1997.

The normalized spectra comparisons show that there is a considerable overlapping of the possible ranges of spectral shapes for different site condition groups. Especially, there is a consistency in corner periods between this study and UBC1997. However, when Figure 4.24 is taken into consideration, the smooth spectral shape for rock and soil sites determined from the UBC 1997 is considerably higher at intermediate periods than the mean curves determined in this study, indicating that proposed curves are not by any means conservative. The generally good agreement between all these curves gives support to estimated corner periods and spectrum shape for the low frequencies for soft soil, soil and rock conditions.

In spite of these similarities between site-dependent response spectra given in UBC 1997 and in this study, regional differences in a wide range of source and propagation parameters indicate that ground-motion relations for specific earthquakes in one region cannot be simply modified for use in engineering applications and analyses in another region. In summary, the UBC definition of the spectrum shape appears to match the shapes derived in this study better.

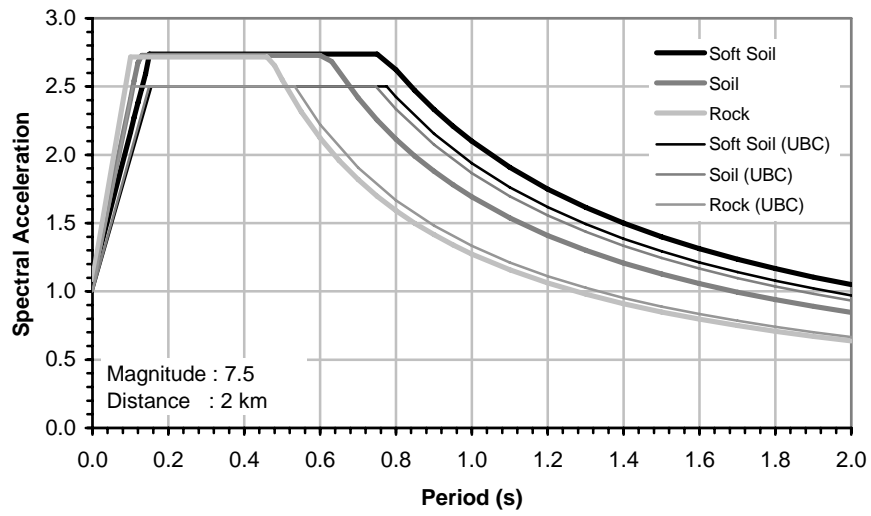


Figure 4.22 Comparison of normalized spectra for 5 percent of critical damping for different site conditions at distance of 2 km

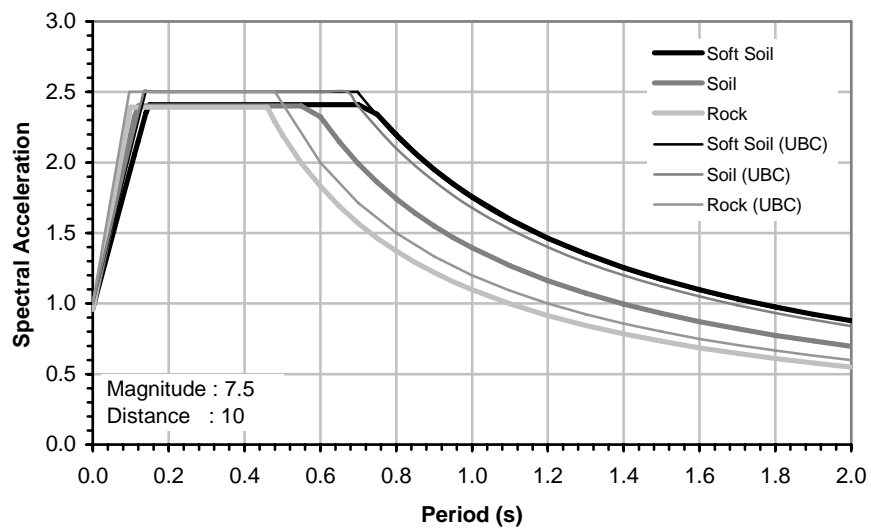


Figure 4.23 Comparison of normalized spectra for 5 percent of critical damping for different site conditions at distance of 10 km

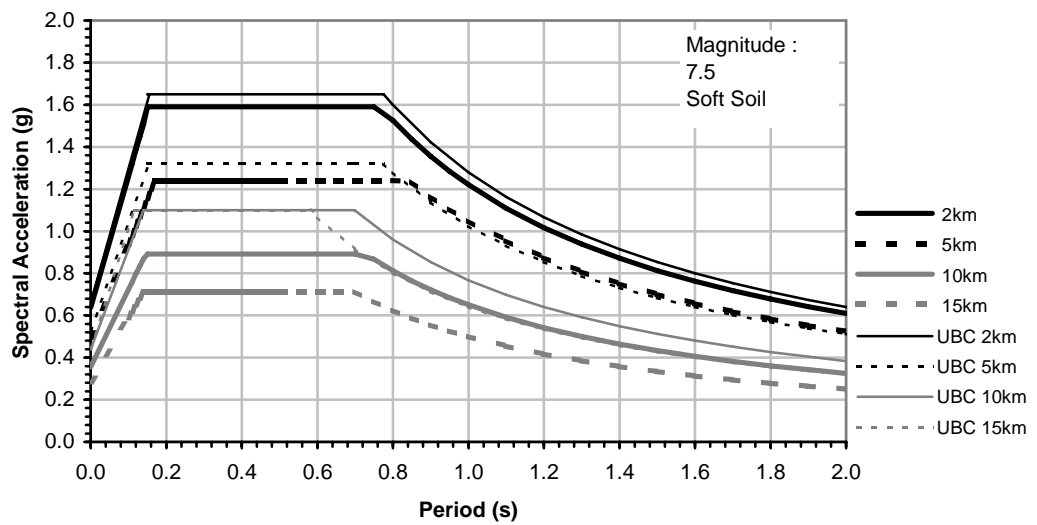
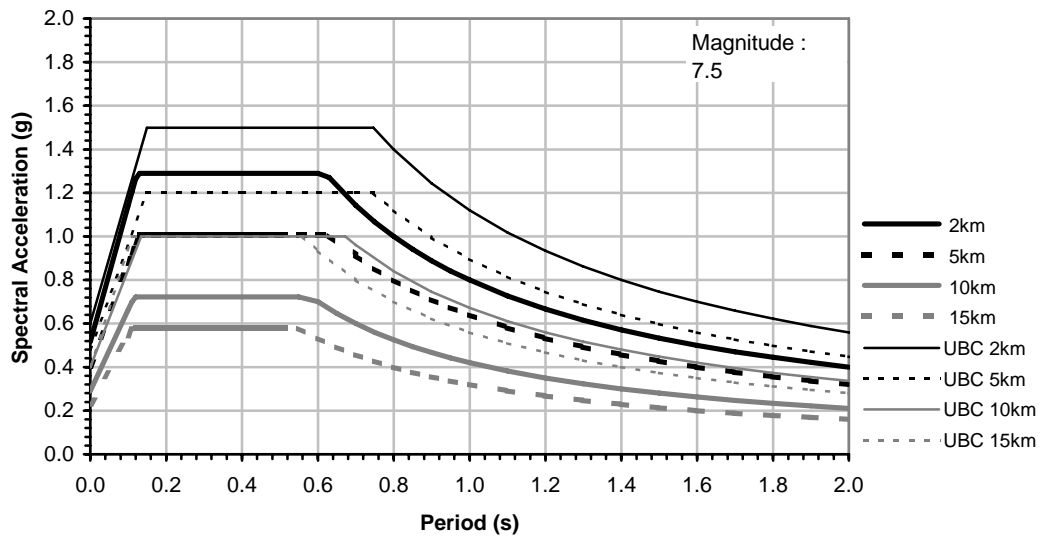
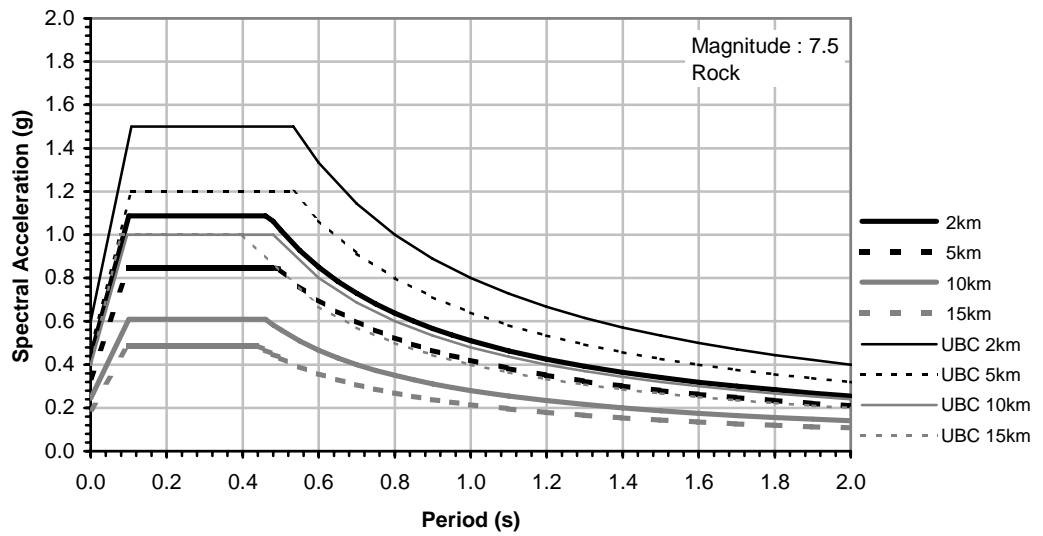


Figure 4.24 Comparison of smooth spectra for 5 percent of critical damping for rock, soil and soft soil conditions at various distances

CHAPTER 5

SUMMARY, CONCLUSIONS AND RECOMMENDATIONS

5.1. SUMMARY

In order to obtain a complete predictive model for the ground motion at a given site, it is necessary first to describe fully the ground motion at the source and next to describe the modifications to the ground motion as it propagates from source to site, i.e., its attenuation. However the nature of source and attenuation are not the same for all regions, hence the appropriate regional descriptions need to be determined for assessing the seismic hazard.

Magnitude is a valid measure to describe the size of the earthquake, however it cannot be directly used for the design of earthquake resistant structures. In earthquake engineering, in order to determine the effects of earthquakes on any structure, earthquake induced ground acceleration, velocity and displacement should be predicted. In this aspect derived attenuation relationships become useful tools. For this aim, many researchers have developed different attenuation relationships for different seismic regions. Most of them are for peak ground acceleration (PGA), because the forces affecting the structure due to an earthquake excitation are directly related to the acceleration of the ground motion. This practice was also followed in this study and the proposed predicting equations are based on peak ground acceleration values. The relationships were derived in a similar form to those previously developed by Boore et al. (1997) for shallow earthquakes in western North America.

In this study, compiled strong motion records taken from the past earthquake database which was supplemented by the information collected from the fault types of earthquakes, soil condition of the recording stations and distances from the fault rupture to the monitoring stations. At the end, empirical equation for predicting strong ground motion was typically fit to this strong motion data set by performing nonlinear regression analysis.

As an output of these analyses, a consistent set of empirical attenuation relationships are presented for predicting free field horizontal component of peak ground acceleration (PGA), and 5% damped pseudo-absolute spectral acceleration (PSA) with their uncertainties including their probable sources. These results were used for the development of 5 percent damped site-dependent response spectra for Turkey and those proposed spectra were also compared with current seismic provisions, including Turkish Seismic Code (1998) and UBC (1997).

5.2. DISCUSSION AND CONCLUSIONS

The following discussion and conclusions can be drawn from the results of this study:

- The recommended attenuation relationships presented in detail in this dissertation through Table 3.1 and illustrated in Figures 3.1 through 3.9 are considered to be appropriate for the estimation of horizontal components of peak ground acceleration, and 5 percent damped pseudo spectral acceleration for earthquakes with magnitude in the range of (M_w) 5 to 7.5 and $r_{cl} < 150$ km for soft soil, soil and rock site conditions in active seismic regions of Turkey.
- There are only a few recordings in our data set for distances greater than 100 km, and so it should be recommended that the equations should not be used for longer distances. Such a limitation is inherent in the strong-motion data set as long as conventional triggered instruments dominate it.

- Although commonly used amplitude parameters include peak acceleration, peak velocity, and peak displacement, this study has mainly focused on peak horizontal acceleration values. Actually, the peak acceleration provides a good indication of the high-frequency component of a ground motion. The peak velocity and peak displacement describe the amplitudes of the intermediate and low frequency components, respectively.
- The database from which these estimates have been drawn is not pristine. It is handicapped not only because of the sheer dearth of records but also because of their poor distribution, arbitrary location, near-total lack of knowledge of local geology, and possible interference from the response of buildings where the sensors have been stationed.
- Aftershock data have been excluded and records with peaks of less than about 0.04 g have been omitted. It is shown in Table A.1, that more than half of the records have been recovered from two M_w 7+ events that occurred in 1999. Inevitably, the regression expressions are heavily imbued with that data proper. A point of generalization is that, in general, the database causes larger margins of error in the estimates. This is more noticeable for spectral accelerations at longer periods.
- It is a truism that, as additional strong motion records, shear wave velocity profiles for recording sites, and better determined distance data become available for Turkey, the attenuation relationships derived in this study can be progressively modified and improved, and their uncertainties reduced.
- There are different ways in which relationship derived differs from those of most other authors. These differences are judged to be reasonable because different databases, regression models and analysis methods, different definitions for source to site distance and magnitude parameters among the relationships are contained in each model. Besides these differences,

performed comparisons between derived attenuation relationship results and other recent attenuation relationship results once again show that ground motion relationships obtained from earthquakes in one region cannot be simply used in engineering analysis in another region.

- The study also presents the results of a statistical analysis of 47 ground-motion records obtained from 19 earthquakes for the development of site-dependent response spectra for Turkey. The analysis shows clear differences in spectral shapes for different soil and geological conditions, indicating the need for consideration of these effects in selecting earthquake-resistant design criteria. The spectral forms presented in Figure 4.11 through Figure 4.13 might serve as a useful guide for selecting site-dependent ground motion characteristics for design purposes.
- Attenuation formulations are commonly used in many research and earthquake hazard programs. One of the research programs using this type of prediction formula is ‘Procedures for Developing Hazus-Compatible Building-Specific Damage and Loss Functions’ this research program was performed for National Institute of Building Services and Federal Emergency Management Agency in 1999 [27]. This is given here just as an example for the reader, in the future the presented estimate equations in this study can be reliably used in Turkey for other earthquake hazard mitigating studies.

5.3. FUTURE RECOMMENDATIONS

This dissertation has presented the derivation of attenuation relationships and site-dependent response spectra with their use in earthquake engineering applications. In this study for the process of regression analysis, the shear velocities are assumed values rather than in-situ measures, because there are no such measurements performed for most of the strong ground motion recording stations in Turkey. Predictions are made according to the reported soil conditions of these

stations. This is one of the unavoidable causes of uncertainties in this study. In the future, in order to eliminate these errors originated from suspicious information about geological conditions and to acquire reliable information on the consequences of earthquakes, proper shear wave velocity measurements should be performed for each and every recording station.

Additionally, strong motion recordings have started to taken in Turkey since 1975, this causes limited number of strong earthquakes having a magnitude greater than 5.0. In that connection, it is of interest to note that given attenuation relationships were derived by using 19 events and the moment magnitude of two of these were 4.5 and 4.9, respectively. For that reason, the number of stations in strong motion network might be increased to enrich the strong motion database. There are other attributes that must be mentioned. Earthquake data were recorded mostly in small buildings built as meteorological stations up to three stories tall because the strong motion stations in Turkey are co-located with institutional facilities for ease of access, phone hook-up and security. This causes modified acceleration records. In order to eliminate these soil-structure interaction effects on digital records and obtain more reliable data sets the recording instruments should be isolated from these buildings and turned into free-field stations.

REFERENCES

- [1] Hanks T.C., and Kanamori H., A Moment Magnitude Scale, *J. Geophysics. Res.*, Vol. 84, No. 2, pp. 348-2,350, 1979.
- [2] Naeim F., *The Seismic Design Handbook*, 1989.
- [3] Kramer S.L., *Geotechnical Earthquake Engineering*, Prentice Hall, 1996.
- [4] Wells D.L., Coppersmith K.J., New Empirical Formula Among Magnitude, Rupture Length, Rupture Width, Rupture Area, and Surface Displacement, *Bulletin of Seismological Society of America*, Vol. 84, No. 4, pp. 974-1002, August 1994.
- [5] Marmara ve Düzce Depremleri Mühendislik Raporu, ODTÜ–TMMOB, Ankara, April 2000.
- [6] Campbell K.W., Predicting Strong Ground Motion in Utah, in Gori, P.L. and W.W. Hayf, eds., *Assessment of Regional Earthquake Hazards and Risk Along The Wasatch Front, Utah, U.S. Geological Survey Open-file Report 87-585*, II, L1-L90, 1987.
- [7] Campbell K.W., Empirical Prediction Near-Source Ground Motion for The Diablo Canyon Power Plant Site San Luis Obispo County, California, *U.S. Geological Survey Open File Report*, pp. 89-484, 1989a.

- [8] Campbell K.W., The Dependence of Peak Horizontal Acceleration on Magnitude, Distance, and Site Effects for Small-Magnitude Earthquakes in California and Eastern and North America, *Bulletin of Seismological Society of America*, Vol. 79, No. 1, pp. 311-1,346, 1989b.
- [9] United States Geological Survey (USGS), National Earthquake Information Center, http://geohazards.cr.usgs.gov/html_files/turkey
- [10] Boore D.M., Joyner W.B., Fumal T.E., Equations for Estimating Horizontal Response Spectra and Peak Acceleration from Western North American Earthquakes: A Summary of Recent Work, *Seismological Research Letters*, Vol. 68, No. 1, pp.128-153, January/February 1997.
- [11] Bates D.M., Watts D.G., *Nonlinear Regression Analysis and Its Applications*, 1988.
- [12] SPSS, Inc. SPSS Ver. 9.0, Chicago, IL, 1998.
- [13] Joyner B.W., Boore M.D., Methods for Regression Analysis of Strong-Motion Data, *Bulletin of Seismological Society of America*, Vol. 83, No. 2, pp. 469-487, April 1993.
- [14] Şıklar E., *Regrasyon Analizine Giriş*, Anadolu Üniversitesi, Eskişehir, 2000.
- [15] Campbell K.W., Empirical Near Source Attenuation Relationships for Horizontal and Vertical Components of Peak Ground Acceleration, Peak Ground Velocity, and Pseudo-Absolute Acceleration Response Spectra, *Seismological Research Letters*, Vol. 68, No. 1, pp. 154-179, January/February 1997.

- [16] Sadigh K., Chang C.Y., Egan J.A., Makdisi F., Youngs R.R., Attenuation Relationships for Shallow Crustal Earthquakes Based on California Strong Motion Data, *Seismological Research Letters*, Vol. 68, No. 1, pp. 180-189, January/February 1997.
- [17] Spudich P., Fletcher J.B., Hellweg M., A New Predictive Relation for Earthquake Ground Motions in Extensional Tectonic Regimes, *Seismological Research Letters*, Vol. 68, No. 1, pp. 190-198, January/February 1997.
- [18] Ambraseys N.N., Simpson K.A, and Bommer, J.J., Prediction of Horizontal Response Spectra in Europe, *Earthquake Engineering and Structural Dynamics*, Vol. 25, No. 4, pp. 371-400, 1996.
- [19] Atkinson G.M., Boore D.M., Some Comparisons between Recent Ground Motion Relations, *Seismological Research Letters*, Vol. 68, No. 1, pp. 24-40 January/February, 1997.
- [20] Toro R.G., Abrahamson N.A., Schneider J.F., Model of Strong Ground Motions from Earthquakes in Central and Eastern North America: Best Estimates and Uncertainties, *Seismological Research Letters*, Vol. 68, No. 1, pp. 41-57 January/February, 1997.
- [21] Housner G.W., An Investigation of the Effects of Earthquakes on Buildings, Ph.D. Thesis California Institute of Technology, Pasadena, CA, 1941.
- [22] Biot, M.A., Analytical and Experimental Methods in Engineering Seismology, *Proc. ASCE*, January 1942.
- [23] Newmark, N.M. and Hall, W.J., Procedures and Criteria for Earthquake Resistant Design, Building Practices for Disaster Mitigation, National Bureau

of Standards, U.S. Department of Commerce, *Building Research Series*, Vol. 46, pp. 209-236, 1973.

- [24] Chopra A.K., *Dynamics of Structures*, New Jersey, 1995.
- [25] FEMA-273, *NEHRP Guidelines for The Seismic Rehabilitation of Buildings*, October 1997.
- [26] Ministry of Public Works and Settlement, *Specification for Structures to be Built in Disaster Areas*, Ankara, 1998.
- [27] National Institute of Building Services, *Procedures for Developing Hazus-Compatible Building-Specific Damage and Loss Functions*, Charles Kircher & Associates, Washington D.C., May 1999.

APPENDIX A

DETAILS OF STRONG MOTION DATABASE

Table A.1 Records used in the development of the attenuation equations for peak horizontal acceleration and spectral accelerations

Date	Earthquake	M_w	r_{cl} (km)	Recording Station	Station Coordinates	Station Site Class	Peak Hor. Acc. (mg)	
							N-S	E-W
19.08.1976	DENİZLİ	5.3	15.20	Denizli: Meteoroloji İstasyonu	37.8140N- 29.1120E	Soil	348.53	290.36
05.10.1977	ÇERKEŞ	5.4	46.00	Çerkeş: Meteoroloji İstasyonu	40.8800N- 32.9100E	Soft Soil	36.03	38.94
16.12.1977	İZMİR	5.5	1.20	İzmir: Meteoroloji İstasyonu	38.4000N- 27.1900E	Soft Soil	391.41	125.40
18.07.1979	DURSUNBEY	5.3	10.30	Dursunbey: Kandilli Gözlem İstasyonu	39.6700N- 28.5300E	Rock	232.29	288.25
05.07.1983	BİGA	6.0	57.70	Edincik: Kandilli Gözlem İstasyonu	40.3600N- 27.8900E	Rock	53.44	46.51
05.07.1983	BİGA	6.1	48.70	Gönen: Meteoroloji İstasyonu	40.0800N- 27.6800E	Soft Soil	50.11	46.77
05.07.1983	BİGA	6.2	75.00	Tekirdağ: Meteoroloji İstasyonu	40.9600N- 27.5300E	Rock	29.89	34.91
30.10.1983	HORASAN-NARMAN	6.5	25.00	Horasan: Meteoroloji İstasyonu	40.0400N- 42.1700E	Soft Soil	150.26	173.30
29.03.1984	BALIKESİR	4.5	2.40	Balıkesir: Meteoroloji İstasyonu	39.6600N- 27.8600E	Soft Soil	223.89	128.97
12.08.1985	KIĞI	4.9	80.77	Kığı: Meteoroloji İstasyonu	39.3400N- 40.2800E	Soil	163.06	89.09
05.05.1986	MALATYA	6.0	29.63	Gölbaşı: Devlet Hastanesi	37.7810N- 37.6410E	Rock	114.70	76.04
06.06.1986	SÜRGÜ (MALATYA)	6.0	34.70	Gölbaşı: Devlet Hastanesi	37.7810N- 37.6410E	Rock	68.54	34.43
20.04.1988	MURADIYE	5.0	37.30	Muradiye: Meteoroloji İstasyonu	39.0300N- 43.7000E	Rock	49.50	51.18
13.03.1992	ERZİNCAN	6.9	65.00	Refahiye: Kaymakamlık Binası	39.9010N- 38.7690E	Soft Soil	67.21	85.93
13.03.1992	ERZİNCAN	6.9	5.00	Erzincan: Meteoroloji İstasyonu	39.7520N- 39.4870E	Soil	404.97	470.92
06.11.1992	İZMİR	6.1	41.00	Kuşadası: Meteoroloji İstasyonu	37.8610N- 27.2660E	Soft Soil	83.49	71.80
24.05.1994	GİRİT	5.4	20.10	Foça: Gümrük Müdürlüğü	38.6400N- 26.7700E	Rock	36.06	49.80
13.11.1994	KÖYCEĞİZ	5.2	17.41	Köyceğiz: Meteoroloji İstasyonu	36.9700N- 28.6940E	Soft Soil	72.79	96.51
01.10.1995	DİNAR	6.4	3.00	Dinar: Meteoroloji İstasyonu	38.0600N - 30.1500E	Soft Soil	288.30	269.95

Table A.1 Continued

Date	Earthquake	M _W	r _{cl} (km)	Recording Station	Station Coordinates	Station Site Class	Peak Hor. Acc. (mg)	
							N-S	E-W
01.10.1995	DİNAR	6.4	46.20	Çardak: Sağlık Ocağı	37.8250N- 29.6680E	Soil	65.07	61.30
27.06.1998	ADANA-CEYHAN	6.3	80.10	Mersin: Meteoroloji İstasyonu	36.8300N- 34.6500E	Soft Soil	119.29	132.12
27.06.1998	ADANA-CEYHAN	6.3	28.00	Ceyhan: PTT Müd.	37.0500N 35.8100E	Soft Soil	223.42	273.55
17.08.1999	KOCAELİ	7.4	55.00	Bursa: Sivil Sav. Müd.	40.1830N- 29.1310E	Soft Soil	54.32	45.81
17.08.1999	KOCAELİ	7.4	81.00	Çekmece: Nükleer Santral Bn.	40.9700N- 28.7000E	Soil	118.03	89.61
17.08.1999	KOCAELİ	7.4	11.00	Düzce: Meteoroloji İstasyonu	40.8500N- 31.1700E	Soft Soil	314.88	373.76
17.08.1999	KOCAELİ	7.4	116.00	Ereğli: Kaymakamlık Bn.	40.9800N- 27.7900E	Soil	90.36	101.36
17.08.1999	KOCAELİ	7.4	15.00	Gebze: Tübitak Marmara Araş. Mer.	40.8200N- 29.4400E	Rock	264.82	141.45
17.08.1999	KOCAELİ	7.4	32.00	Göynük: Devlet Hastanesi	40.3850N- 30.7340E	Rock	137.69	117.9
17.08.1999	KOCAELİ	7.4	49.00	İstanbul: Bayındırlık ve İskan Müd.	41.0580N- 29.0130E	Rock	60.67	42.66
17.08.1999	KOCAELİ	7.4	8.00	İzmit: Meteoroloji İstasyonu	40.7900N- 29.9600E	Rock	171.17	224.91
17.08.1999	KOCAELİ	7.4	30.00	İzmit: Karayolları Şefliği	40.4370N- 29.6910E	Soft Soil	91.89	123.32
17.08.1999	KOCAELİ	7.4	140.00	Kütahya: Sivil Savunma Müd.	39.4190N- 29.9970E	Soil	50.05	59.66
17.08.1999	KOCAELİ	7.4	3.20	Sakarya: Bayındırlık ve İskan Müd.	40.7370N- 30.3840E	Rock	407.04	-
17.08.1999	KOCAELİ	7.4	150.00	Tekirdağ: Hükümet Konağı	40.9790N- 27.5150E	Rock	129.79	128.33
17.08.1999	KOCAELİ	7.4	17.00	Darıca: Arçalık Arge Bn.	40.82360N- 29.3607E	Soil	211.37	133.68
17.08.1999	KOCAELİ	7.4	82.50	Ambarlı: Termik Santrali	40.9809N- 28.6926E	Soft Soil	252.56	186.04
17.08.1999	KOCAELİ	7.4	116.00	M. Ereğlisi: Botaş Gas Terminali	40.9919N- 27.9795E	Soil	98.88	87.10
17.08.1999	KOCAELİ	7.4	72.00	Yeşilköy: Havalimanı	40.9823N- 28.8199E	Soil	90.21	84.47
17.08.1999	KOCAELİ	7.4	63.00	4. Levent: Yapı Kredi Plaza	41.0811N- 20.0111E	Rock	41.08	35.52
17.08.1999	KOCAELİ	7.4	3.28	Yarımca: Petkim Tesisleri	40.7639N-29.7620E	Soil	230.22	322.20
17.08.1999	KOCAELİ	7.4	63.00	Fatih: Fatih Türbesi	41.0196N-28.9500E	Soft Soil	189.39	161.87
17.08.1999	KOCAELİ	7.4	43.00	Heybeliada: Sanatoryum	40.8688N- 29.0875E	Rock	56.15	110.23
17.08.1999	KOCAELİ	7.4	71.00	Bursa: Tofaş Fab.	40.2605N- 29.0680E	Soft Soil	100.89	100.04
17.08.1999	KOCAELİ	7.4	81.00	Çekmece: Nükleer Santral Bn.	40.9700N- 28.7000E	Soil	177.31	132.08
12.11.1999	DÜZCE	7.1	20.41	Bolu: Bayındırlık ve İskan Müd.	40.7450N- 31.6100E	Soft Soil	739.56	805.88
12.11.1999	DÜZCE	7.1	8.23	Düzce : Meteoroloji İstasyonu	40.8500N- 31.1700E	Soft Soil	407.69	513.78
12.11.1999	DÜZCE	7.1	30.90	Mudurnu: Kaymakamlık Binası	40.4630N- 31.1820E	Soft Soil	120.99	58.34

